Left ventricular function

There was a significant dose-related increase of LVEF with carvedilol treatment ($P = .018$), and there was a significantly greater increase of LVEF in the 20 mg group compared with the placebo group ($P = .022$) (Figure 3).

NYHA class and adverse events

A significant dose-dependent improvement of NYHA class was observed with carvedilol treatment (Table V).

The incidence of all serious and nonserious adverse events was lower (but not significantly) in the carvedilol-treated groups (63.3%, 51.1%, and 59.7% in the placebo, 5 mg, and 20 mg groups, respectively). Adverse events with a higher incidence (P = NS) in the 20 mg group were dizziness, upper respiratory tract infections, worsening of diabetes, palpitations, headache, and hypotension.

Discussion

The MUCHA trial demonstrated a dose-related improvement in signs and symptoms of heart failure assessed by the attending physicians and improvement of LVEF in Japanese patients with CHF who received long-term carvedilol therapy at low doses of 5 or 20 mg/d. These low doses achieved a remarkable reduction in the risk of death or CVD hospitalization; surprisingly, the 5 mg/d dose achieved a reduction (71%) that was nearly as great as that for the 20 mg/d dose (80%).

In the current study, a dramatic reduction in the risk of hospitalization for CHF or CVD was observed with both carvedilol regimens. Although the majority of the patients were in NYHA class II, this was probably not the reason for the marked reduction of CVD hospitalization, because previous trials performed in the United States and Australasia[1-3] have shown that risk reduction is not related to the NYHA class.

In the current study, carvedilol reduced the risk of death or CVD hospitalization irrespective of the presence of hypertension, diabetes, hyperlipidemia, and atrial fibrillation. In the CIBIS-II study, the β_1-selective blocking agent bisoprolol decreased mortality and hospitalization rates in patients with sinus rhythm but not in patients with atrial fibrillation.[14] In contrast, we found that carvedilol reduced the risk of death or cardiovascular hospitalization irrespective of the presence of atrial fibrillation, consistent with the results of the US Carvedilol Heart Failure Trials Program.[15]

In previous studies of carvedilol therapy for patients with CHF, improvement of LVEF was accompanied by a reduction of rates for death or CVD hospitalization.[10] At a dose of 5 mg/d, however, a marked reduction in the risk of CVD hospitalization in the current study was observed without a statistically significant improvement of LVEF. In patients with CHF, Quaife et al[16] reported that carvedilol improved the right ventricular ejection fraction, with a decrease of the right ventricular end-diastolic and end-systolic volumes and a decrease of the pulmonary arterial pressure. They also suggested that the improvement of right ventricular systolic function was not secondary to the improvement of left ventricular function but was due to the direct effect of carvedilol.[16] Our results may be consistent with a direct effect of low-dose carvedilol on right ventricular function.

The recommended dose of carvedilol shown by the US MOCHA trial was 12.5 to 50 mg/d and that shown by the MUCHA trial in Japan was 5 to 20 mg/d. Since the pharmacokinetics of carvedilol are similar in healthy Japanese and American adults (unpublished observation), whereas β_1-receptor sensitivity is higher in Chinese than in white or black Americans,[17] the difference in the effective dose between patients in Japan and Western countries may depend on a difference in β_1-receptor sensitivity.

The current findings regarding the global improvement of heart failure, LVEF, and morbidity strongly suggest that the recommended dose of carvedilol for Japanese patients with CHF should range from 5 to 20 mg/d. In addition, our finding of reduced morbidity at a low dose of carvedilol (5 mg/d) suggested that low-dose therapy may have a beneficial effect in patients who cannot tolerate a standard regimen. A future large-scale study will be necessary to evaluate the impact of low-dose, long-term carvedilol therapy on survival in Japanese patients with CHF.

References

1. Packer M, Bristow M, Cohn JN, et al. The effect of carvedilol on morbidity and mortality in patients with chronic heart failure. N Engl J Med 1996;334:1349–55.
2. Australia/New Zealand Heart Failure Research Collaborative Group. Randomized, placebo-controlled trial of carvedilol in patients with congestive heart failure due to ischemic heart disease. Lancet 1997;349:375–80.
3. Packer M, Coats AJS, Fowler MB, et al. Effect of carvedilol on survival in severe chronic heart failure. N Engl J Med 2001;344: 1651–8.
4. CIBIS-II Investigators and Committees. The Cardiac Insufficiency Bisoprolol Study II (CIBIS-II): a randomized trial. Lancet 1999;353: 9–13.
5. MERIT-HF Study Group. Effect of metoprolol CR/XL in chronic heart failure: Metoprolol CR/XL Randomized Intervention Trial in Congestive Heart Failure (MERIT-HF). Lancet 1999;353:2001–07.
6. Hunt SA, Baker DW, Chin MH, et al. ACC/AHA guidelines for the evaluation and management of chronic heart failure in the adult. 2001. American College of Cardiology Web site. Available at: http://www.acc.org/clinical/guidelines/failure/hf-index.htm.

7. Ogihara T, Yoshinaga K, Kamahara Y, et al. Clinical efficacy of carvedilol in severe hypertension. J Cardiovasc Pharmacol 1991; 18(4 Suppl):S69–72.
8. Kishida H, Saito T, Fukuma N, et al. Evaluation of a new vasodilating beta-blocking agent, carvedilol, in exertional angina using Holter monitoring. Jpn Heart J 1990;31:449–60.
9. Colucci WS, Packer M, Bristow MR, et al. Carvedilol inhibits clinical progression in patients with mild symptoms of heart failure. Circulation 1996;94:2800–6.
10. Bristow MR, Gilbert EM, Abraham WT, et al. Carvedilol produces dose-related improvements in left ventricular function and survival in subjects with chronic heart failure. Circulation 1996;94:2807–16.
11. Packer M, Colucci WS, Sackner-Bernstein JD, et al. Double-blind, placebo-controlled study of the effect of carvedilol in patients with moderate to severe heart failure: the PRECISE trial: Prospective Randomized Evaluation of Carvedilol on Symptoms and Exercise. Circulation 1996;94:2793–9.
12. Cohn JN, Fowler MB, Bristow MR, et al. Safety and efficacy of carvedilol in severe heart failure. J Card Fail 1997;3:173–9.
13. ICH guideline E9 statistical principles for clinical trial. Published in the Federal Register, Vol. 63, No. 179, September 16, 1998, page 49583, in force September 1998.
14. Lechat P, Hulot JS, Escolano S, et al. Heart rate and cardiac rhythm relationships with bisoprolol benefit in chronic heart failure in CIBIS II trial. Circulation 2001;103:1428–33.
15. Joglar JA, Acusta AP, Shusterman NH, et al. Effect of carvedilol on survival and hemodynamics in patients with atrial fibrillation and left ventricular dysfunction: retrospective analysis of the US Carvedilol Heart Failure Trials Program. Am Heart J 2001;142:498–501.
16. Quaife RA, Christian PE, Gilbert EM, et al. Effect of carvedilol on right ventricular function in chronic heart failure. Am J Cardiol 1998;81:247–50.
17. Xie HG, Kim RB, Wood AJJ, et al. Molecular basis of ethnic differences in drug disposition and response. Annu Rev Pharmacol Toxicol 2001;41:815–50.

Appendix

Executive Committee

S. Hosoda (Chairman), S. Sasayama, M. Hori, A. Kitabatake, T. Toyo-oka, S. Handa, M. Yokoyama, M. Matsuzaki, A. Takeshita, H. Origasa, and K. Matsui.

End Point Committee

S. Handa (Chairman), T. Toyo-oka, T. Izumi, S. Momomura, and K. Kawana.

Data and Safety Monitoring Board

K. Kato (Chairman), T. Serizawa, I. Yamaguchi, K. Mizuno, and H. Origasa.

Available online at www.sciencedirect.com

SCIENCE DIRECT®

European Journal of Pharmacology 505 (2004) 67–74

www.elsevier.com/locate/ejphar

Ursodeoxycholic acid inhibits endothelin-1 production in human vascular endothelial cells

Ji Ma[a,b], Haruko Iida[a], Taisuke Jo[a], Haruhito Takano[a], Hitoshi Oonuma[a], Toshihiro Morita[a], Teruhiko Toyo-oka[a], Masao Omata[a], Ryozo Nagai[a], Yukichi Okuda[b], Nobuhiro Yamada[b], Toshiaki Nakajima[a,c,*]

[a]*Department of Cardiovascular Medicine, Respiratory Medicine, and Gastroenterology, University of Tokyo, 7-3-1 Hongo, Bunkyo-ku, Tokyo 113-8645, Japan*
[b]*Department of Internal Medicine, Institute of Clinical Medicine, University of Tsukuba, 1-1-1 Tennodai, Ibaraki-ken 305-0005, Japan*
[c]*Department of Circulatory Physiology, University of Tokyo, 7-3-1 Hongo, Bunkyo-ku, Tokyo 113-8645, Japan*

Received 5 July 2004; received in revised form 13 October 2004; accepted 14 October 2004
Available online 30 October 2004

Abstract

Endothelin-1 is known to be implicated in the pathogenesis of hepatobiliary diseases such as cirrhosis, especially in portal hypertension. This study aimed to investigate the effects of ursodeoxycholic acid on endothelin-1 production in human endothelial cells. The effects of ursodeoxycholic acid and its conjugates (tauroursodeoxycholic and glycoursodeoxycholic acids) on endothelin-1 production as well as nitric oxide (NO) in human umbilical vein endothelial cells (HUVECs) were examined. The production of endothelin-1 and nitric oxide in culture medium was measured using enzyme-linked immunosorbent assay (ELISA) and the Griess method, respectively. Endothelin-1 and endothelial nitric oxide synthase (eNOS) mRNA expression were investigated by real-time quantitative reverse transcriptase/polymerase chain reaction (RT-PCR). Ursodeoxycholic acid (30–1000 μM) inhibited endothelin-1 production in a concentration-dependent manner, and ursodeoxycholic acid at concentrations higher than 300 μM increased nitric oxide production in culture medium. The conjugates of ursodeoxycholic acid also increased nitric oxide production and decreased endothelin-1 production, which was less effective than ursodeoxycholic acid. *N*-nitro-L-arginine-mythel-ester (L-NAME), a nitric oxide synthase (NOS) inhibitor, suppressed the ursodeoxycholic acid-induced nitric oxide production, but it did not antagonize the inhibitory effects of ursodeoxycholic acid on endothelin-1 production. Ursodeoxycholic acid also induced a concentration-dependent decrease in endothelin-1 mRNA expression without significant changes in eNOS mRNA expression. These results provide novel evidence that ursodeoxycholic acid inhibits endothelin-1 production in human endothelial cells, but nitric oxide is not responsible for the inhibitory effect of ursodeoxycholic acid on endothelin-1. Thus, ursodeoxycholic acid therapy may prevent the development of several pathogenesis such as portal hypertension observed in patients with cirrhosis due to the improvement of endothelial function.

Keywords: Ursodeoxycholic acid; Human endothelial cell; Endothelin-1; Nitric oxide; Real-time RT-PCR

1. Introduction

Endothelin-1, a 21-amino-acid peptide (Yanagisawa et al., 1988), is synthesized by various cells including hepatic and endothelial cells. It has been known to be a potent vasoconstrictor and mitogen for vascular smooth muscle cells in the liver (Gandhi et al., 1990; Serradeil-Le Gal et al., 1991), which is implicated in the pathogenesis of a variety of diseases such as hepatobiliary diseases (Tsai et al., 1995; Alam et al., 2000; Shah, 2001). Endothelin-1 is overexpressed in cirrhotic tissues (Pinzani et al., 1996; Kuddus et al., 2000; Tieche et al., 2001), and endothelin-1 level is elevated in patients or animal models with cirrhosis, especially in portal hypertension (Moller et al., 1995; Bernardi et al., 1996; Bruno et al., 2000). The increased expression of endothelin-1 mRNA and the subsequent increase in production has been

* Corresponding author. Department of Cardiovascular Medicine, Respiratory Medicine, and Gastroenterology, University of Tokyo, 7-3-1 Hongo, Bunkyo-ku, Tokyo 113-8645, Japan. Tel.: +81 3 3815 5411; fax: +81 3 3814 0021.
E-mail address: masamasa@pb4.so-net.ne.jp (T. Nakajima).

0014-2999/$ - see front matter © 2004 Elsevier B.V. All rights reserved.
doi:10.1016/j.ejphar.2004.10.042

also reported in the experimental models of liver injury and cirrhotic rats (Leivas et al., 1995; Rockey et al., 1998).

On the other hand, nitric oxide (NO), derived from endothelium or other cells, also plays a vital role in regulating vascular tone (Moncada et al., 1991; Nathan, 1992), and it is another important physiological and pathophysiological mediator in hepatobiliary diseases. Nitric oxide is synthesized from L-arginine by isoforms of nitric oxide synthase (NOS). Nitric oxide released from endothelial nitric oxide synthase (eNOS) is a physiologically potent vasodilator and an inhibitor of vascular smooth muscle cell proliferation, which is considered to have a beneficial role. In fact, diminution in eNOS-derived nitric oxide production in liver has been reported to be involved in development of portal hypertension by increasing intrahepatic resistance (Shah, 2001). And 2-(acetyloxy)benzoic acid 3-(nitrooxymethyl)phenyl ester (NCX-1000), a nitric oxide-releasing derivative of ursodeoxycholic acid, selectively divers nitric oxide to the liver and protects against development of portal hypertension (Fiorucci et al., 2001).

Ursodeoxycholic acid, a hydrophilic tertiary bile acid, has been wildly used to treat patients with chronic cholestatic liver diseases (Luketic and Sanyal, 1994) and has benefits for the treatment in patients with various liver diseases such as primary biliary cirrhosis and chronic viral hepatitis (Cirillo and Zwas, 1994; Makino and Tanaka, 1998). Ursodeoxycholic acid also inhibits progression of chronic hepatic disorders with special reference to increases in blood flow and limits the development of portal hypertension induced by bile duct ligation (Poo et al., 1992; Poo et al., 1995). The basic mechanism has not yet been identified, but a wide range of cellular actions of ursodeoxycholic acid, i.e., anti-inflammatory and immunomodulating effects (Makino and Tanaka, 1998; Ma et al., 2003), has been proposed. It also protects hepatocytes against oxidant injury via induction of antioxidants (Mitsuyoshi et al., 1999). In human vascular endothelial cells, we have reported that bile acids such as chenodeoxycholic acids increase nitric oxide production by increasing intracellular Ca^{2+} concentration $[Ca^{2+}]_i$ (Nakajima et al., 2000; Chisaki et al., 2001), but the effects of ursodeoxycholic acid on endothelin-1 production have not been investigated.

In the present study, the effects of ursodeoxycholic acid on endothelin-1 production as well as nitric oxide in human endothelial cells were investigated. Here, we provided novel evidence that ursodeoxycholic acid inhibits endothelin-1 production in human umbilical vein endothelial cells (HUVECs), but nitric oxide is not responsible for ursodeoxycholic acid effects on endothelin-1.

2. Materials and methods

2.1. Materials

HUVECs were purchased from BioWhittaker and cultured in endothelial growth medium (EGM) supplemented with 0.1% human epithelial growth factor, 0.1% hydrocortisone, 0.1% Gentamicin sulfate Amphotericin (GA1000), 0.4% bovine brain extract, 2.0% fetal bovine serum in an atmosphere of 5% CO_2, and 95% air at 37 °C in 25-cm^2 flasks. At confluence, cells were split 1:3 after they were detached using 0.25% trypsin in 0.02% EDTA. Media were changed twice weekly. The confluent cells were used within 3 weeks of establishing primary cultures and at the third to fifth passage.

Ursodeoxycholic acid (Na salt), tauroursodeoxycholic acid (Na salt), and glycoursodeoxycholic acid (Na salt) were kindly provided by Mitsubishi Pharma (Osaka, Japan). *N*-nitro-L-arginine-mythel-ester (L-NAME) was purchased from Sigma (St. Louis, MO).

2.2. Determination of nitric oxide

Nitric oxide released from HUVECs was determined by measuring the concentration of NO_2^-, a stable metabolite of nitric oxide, in culture medium, using the Griess method, as described previously (Nakajima et al., 2000; Ma et al., 2003). Confluent monolayers cultured in 35-mm dishes were washed twice with phosphate buffered saline (pH 7.4), and then, 2 ml of the EGM supplemented with or without various concentrations of ursodeoxycholic acid or the conjugated bile acids (tauroursodeoxycholic and glycoursodeoxycholic acids) were added. Two hours later, 1.5-ml aliquots of cultured medium were collected and centrifuged for 2 min at 12,000 $\times g$. One milliliter of Griess reagent (0.5% naphthylethylenediamine dihydrochloride and 5% sulphanilamide in 25% H_3PO_4) was added to 1 ml supernatant, and the mixture was incubated at room temperature for 10 min. The absorbance at 540 nm was measured in a Beckman DU-70 spectrophotometer (Fullerton, CA). The concentration of NO_2^- was calculated by comparison with the absorbance at 540 nm of standard solutions of 0–150 μM $NaNO_2$ prepared in the EGM.

2.3. Measurement of endothelin-1 concentration

The amount of endothelin-1 produced by HUVECs was determined by measuring the concentration of endothelin-1 in cultured medium, using enzyme-linked immunosorbent assay (ELISA) Kit (TECHNE, Minneapolis, MN). Diluted conjugate (100 μl; antibody to endothelin-1 conjugated to horseradish peroxidase) was added to each endothelin-1 antibody-precoated well. Then 100 μl supernatant (above-mentioned in nitric oxide determination) or standard solution was added to each well with sufficient force to ensure mixing and was incubated at room temperature for 30 min. Afterwards, the content from each well was aspirated and washed with wash buffer (buffered surfactant). Substrate (100 μl; tetramethylbenzidine) was added to each well and was incubated at room temperature for 30 min. Then, 100 μl stop solution (acid solution) was added to each well. The optical density of each well was determined using

a biolumin 960 microplate reader (Molecular Dynamics Japan, Tokyo) set at 450 nm, with the correction wavelength set at 620 nm. The concentration of endothelin-1 was calculated by comparison with standard solutions containing 0–150 pg/ml endothelin-1 prepared in the EGM.

2.4. Protein assay

After HUVECs proliferated to confluence in 35-mm dishes, the cells were washed three times in a HEPES buffered saline solution and then lysed in 0.5 M NaOH. The protein content of the cytolysate of the total cells was measured by the Bradford protein assay.

2.5. RNA extraction and real-time quantitative reverse transcriptase/polymerase chain reaction (RT-PCR)

Total RNAs were isolated as described above (Jo et al., 2004) and then treated with DNase I. They were then converted to cDNAs, using a Super Script first-strand synthesis system (Invitrogen). Quantitative RT-PCR was performed with the use of real-time Taq-Man technology and a sequence detector (model 7700, Applied Biosystems, Foster City, CA). Gene-specific primers and Taq-Man probes (endothelin-1, accession no. NM 001955; eNOS, accession no. NM 000603) were used to analyze the transcript abundance. The 18 S ribosomal RNA was analyzed as an internal control and was used to normalize the values for the transcript abundance.

2.6. Statistical analysis

Statistical comparison was carried out with three or more groups using one-way analysis of variance and Dunnett's test. Data are expressed as the mean±S.E.M., and values of $p<0.05$ were considered statistically significant.

3. Results

3.1. Effects of ursodeoxycholic acid on endothelin-1 and nitric oxide production

Fig. 1 shows the effects of ursodeoxycholic acid on the production of endothelin-1. The amount of endothelin-1 (pg/ml) released from HUVECs for 2 h in the culture medium under the control medium and in the presence of various concentrations of ursodeoxycholic acid (30–1000 μM) is shown in Fig. 1. Compared with the control solution, ursodeoxycholic acid decreased the production of endothelin-1 in the culture medium in a concentration-dependent manner. Significant inhibitory effects of ursodeoxycholic acid were observed at concentrations above 30 μM. The basal endothelin-1 release for 2 h was 52±4 (n=6) and 245±24 pg/mg (n=6). The addition of ursodeoxycholic acid in the culture medium decreased the endothelin-1 production (46±2 and 214±20 pg/mg ($p<0.05$, n=6) at 100 μM; and 41±3 and 196±11 pg/mg ($p<0.01$, n=6) at 300 μM; and 35±4.7 and 181±16 pg/mg ($p<0.01$, n=6) at 500 μM).

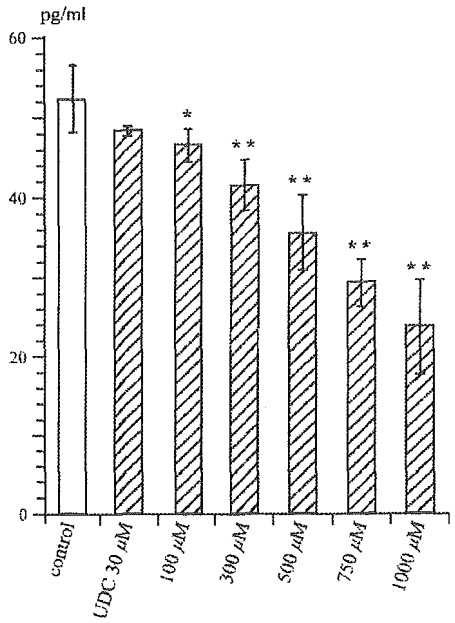

Fig. 1. Effects of ursodeoxycholic acid on the production of endothelin-1 in human umbilical vein endothelial cells (HUVECs). The cells were treated with or without various concentrations of ursodeoxycholic acid (UDC) for 2 h. The amount of endothelin-1 (pg/ml) in the culture medium released from HUVECs was measured and plotted against each concentration of UDC (30–1000 μM). Note that UDC inhibits endothelin-1 production in a concentration-dependent manner. The data represent mean±S.E.M of six different experiments. *$p<0.05$, **$p<0.01$ vs. control.

Fig. 2 illustrates the effects of ursodeoxycholic acid for 2 h on nitric oxide production. The concentration of NO_2^- in the culture medium was measured in the control and the presence of various concentrations of ursodeoxycholic acid (30–1000 μM). Ursodeoxycholic acid at concentrations more than 300 μM significantly increased nitric oxide production. The production of NO_2^- under the control medium for 2 h was 0.55±0.06 μM (n=6) and 2.5±0.3 μM/mg (n=6). The addition of ursodeoxycholic acid in the culture medium increased the NO_2^- production (0.67±0.03 μM, 3.23±0.2 μM/mg ($p<0.05$, n=6) at 300 μM, and 0.82±0.05 μM, 4.01±0.4 μM/mg (n=6, $p<0.01$) at 500 μM).

Figs. 3 and 4 compared the effects of ursodeoxycholic acid and the conjugated bile acids on endothelin-1 (Fig. 3) and nitric oxide (Fig. 4) production. Tauroursodeoxycholic and glycoursodeoxycholic acids as well as ursodeoxycholic acid (500 and 750 μM) increased nitric oxide production in a similar manner (Fig. 4), but they inhibited endothelin-1 production less than ursodeoxycholic acid (Fig. 3).

3.2. Effects of ursodeoxycholic acid on endothelin-1 and eNOS mRNA expression

Fig. 5 shows the effects of ursodeoxycholic acid on endothelin-1 (Fig. 5A) and eNOS (Fig. 5B) mRNA

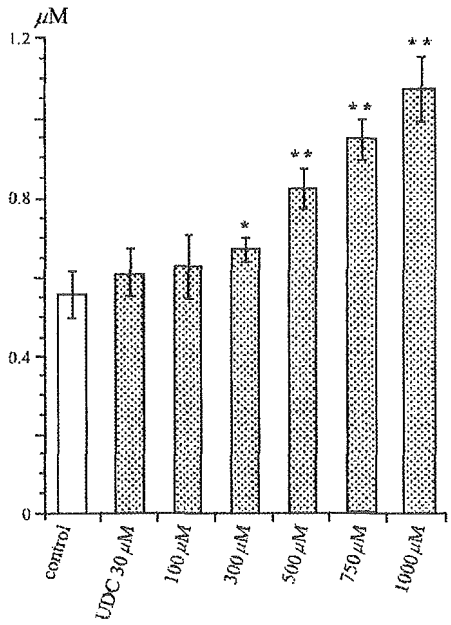

Fig. 2. Effects of ursodeoxycholic acid on the production of nitric oxide in HUVECs. The cells were treated with or without various concentrations of ursodeoxycholic acid (UDC) for 2 h. The concentration of NO_2^- (μM) in the culture medium released from HUVECs was plotted against each concentration of UDC (30–1000 μM). Note that UDC at concentrations higher than 300 μM increases the nitric oxide production. Each column represents the mean±S.E.M of six different experiments. *p<0.05, **p<0.01 vs. control.

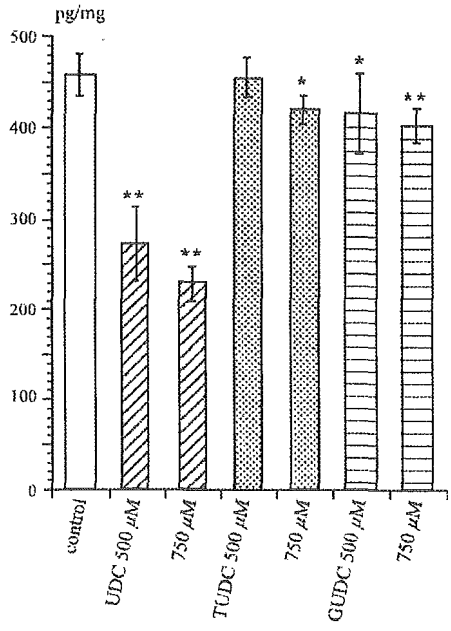

Fig. 3. Effects of ursodeoxycholic acid and the conjugated bile acids on endothelin-1 production. The cells were treated with ursodeoxycholic acid (UDC) or the conjugated bile acids [tauroursodeoxycholic acid (TUDC) and glycoursodeoxycholic acid (GUDC)] for 2 h, and the amount of endothelin-1 released from the cells (pg/mg) was measured and plotted against each concentration of these agents. Each column represents the mean±S.E.M of six different experiments. *p<0.05, **p<0.01 vs. control.

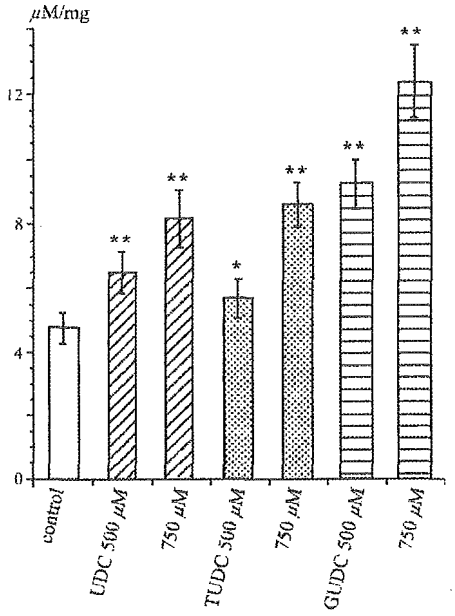

Fig. 4. Effects of ursodeoxycholic acid and the conjugated bile acids on nitric oxide production. The cells were treated with ursodeoxycholic acid (UDC) or the conjugated bile acids [tauroursodeoxycholic acid (TUDC) and glycoursodeoxycholic acid (GUDC)] for 2 h, and the amount of nitric oxide production under these conditions is plotted against each concentration of these drugs. Each column represents the mean±S.E.M of six different experiments. *p<0.05, **p<0.01 vs. control.

expression. The expression of mRNA was compared in cells treated with or without ursodeoxycholic acid (100–750 μM) for 4 h. Ursodeoxycholic acid induced a significant decrease in endothelin-1 mRNA expression. The mean % decrease was 32% of the control at 100 μM, 53% at 300 μM, 91% at 500 μM, and 91% at 750 μM, respectively. On the other hand, ursodeoxycholic acid (100–750 μM) did not modify the iNOS mRNA expression significantly. Similarly, treatment of cells with 500 μM ursodeoxycholic acid for 2 h decreased endothelin-1 mRNA expression to approximately 20% of the control.

3.3. Effects of N-nitro-L-arginine-mythel-ester (L-NAME) on the inhibitory effects of ursodeoxycholic acid on endothelin-1 production

Fig. 6A shows the effects of L-NAME, an inhibitor of nitric oxide synthase, on endothelin-1. The endothelin-1 production was 318±61 pg/mg (n=6) in control, and it was 158±44.7 pg/mg (n=6, p<0.01) at ursodeoxycholic acid (500 μM). The inhibitory effect of ursodeoxycholic acid on endothelin-1 production was not blocked by L-NAME (Fig. 6A, 1 and 2 mM, n=6). The statistical significance was not observed in between ursodeoxycholic acid in the absence of L-NAME and ursodeoxycholic acid in the presence of L-NAME (1 and 2 mM, n=6).

Fig. 6B shows the effects of L-NAME on nitric oxide production. Under the control medium, L-NAME

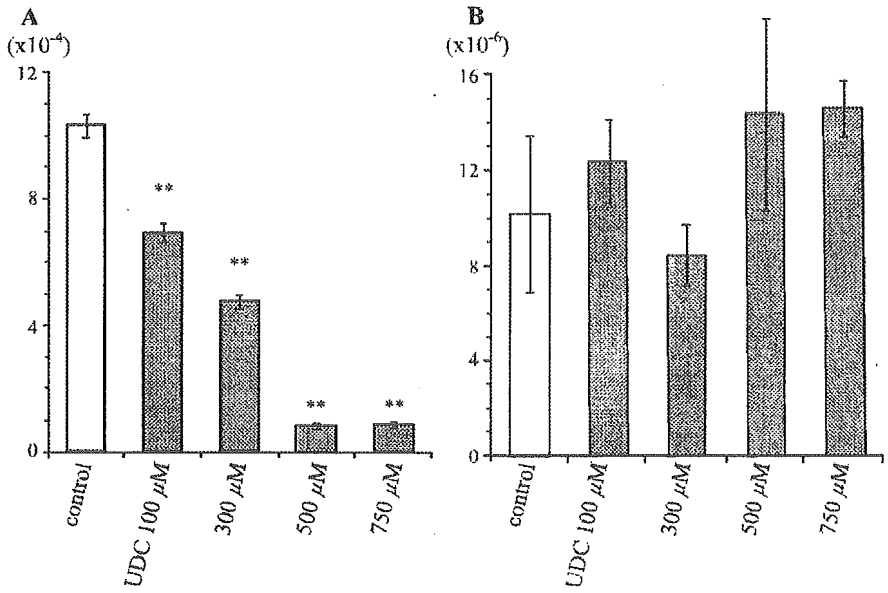

Fig. 5. Effects of ursodeoxycholic acid on endothelin-1 and eNOS mRNA expression. The cells were treated with various concentrations of ursodeoxycholic acid (UDC) for 4 h, and the total RNA was isolated from cells. The expression levels of endothelin-1 (A) and eNOS (B) mRNA were normalized to those of the 18 S ribosomal RNA levels. Data are means±S.E.M from six different samples. $^{**}p<0.01$ vs. control.

decreased nitric oxide production from 3.06±0.5 μM/mg (n=6) in the control to 1.90±0.26 μM/mg (n=6, $p<0.01$) at 1 mM L-NAME, and 2.2±0.17 μM/mg (n=6, $p<0.01$) at 2 mM L-NAME. L-NAME also significantly inhibited the production of NO_2^- induced by ursodeoxycholic acid (Fig. 6B).

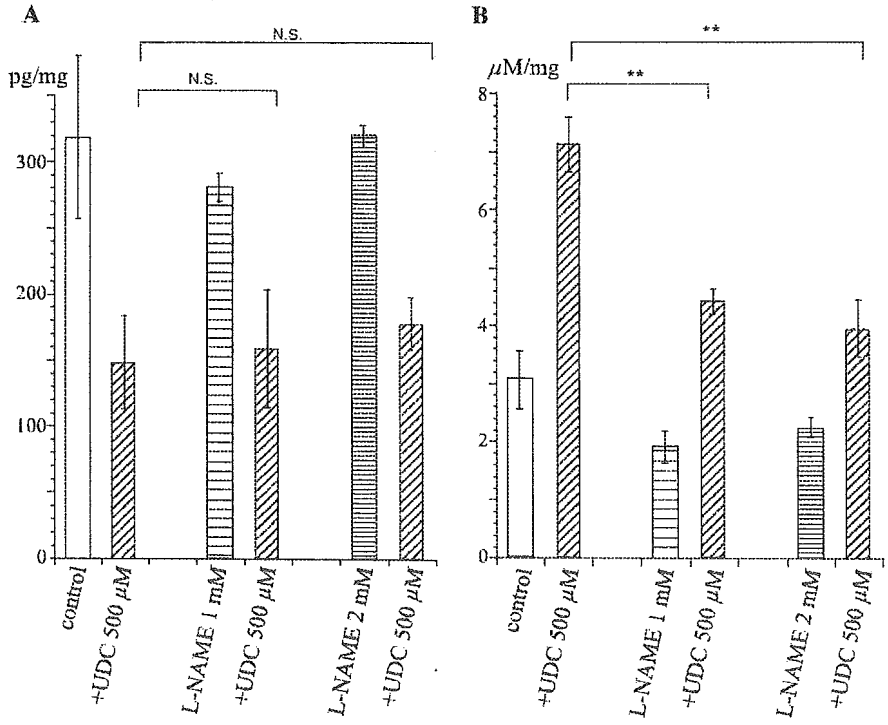

Fig. 6. Effects of L-NAME on the inhibitory effects of ursodeoxycholic acid on endothelin-1 production and the stimulatory effects of ursodeoxycholic acid on nitric oxide production. The cells were treated with or without ursodeoxycholic acid (UDC, 500 μM) in the absence or presence of L-NAME (1 and 2 mM). The amount of endothelin-1 released from the cells for 2 h (pg/mg) were measured and plotted in panel (A). In panel (B), the amount of nitric oxide production under these conditions is plotted. Note that L-NAME inhibits nitric oxide production induced by UDC, but it fails to suppress the inhibitory effects of UDC on endothelin-1 production. Each column represents the mean±S.E.M of six different experiments. $^{**}p<0.01$ vs. UDC in the absence of l-NAME.

4. Discussion

The present study showed novel evidence that ursodeoxycholic acid significantly decreased endothelin-1 mRNA expression and endothelin-1 production in human endothelial cells. Ursodeoxycholic acid at concentrations higher than 300 μM increased nitric oxide production, but the inhibitory effects of ursodeoxycholic acid on endothelin-1 production was not inhibited by a nitric oxide synthase inhibitor, L-NAME. These results suggest that ursodeoxycholic acid inhibits endothelin-1 production in human endothelial cells, but nitric oxide is not responsible for the inhibitory effect of ursodeoxycholic acid on endothelin-1 production.

Several mechanisms may be proposed in the inhibitory effects of ursodeoxycholic acid on endothelin-1 production. The bile acids are known to induce cell damage because of their detergent property. However, as reported previously in human endothelial cells (Garner et al., 1991), the concentration of ursodeoxycholic acid used in the present study did not affect the morphology of HUVECs, and the viability measured by trypan blue excursion was not different in between control cells and cells treated with ursodeoxycholic acid. Thus, it is unlikely that the detergent effects are involved in ursodeoxycholic acid effects on endothelin-1. In addition, we have reported that bile acids such as chenodeoxycholic acid increase intracellular Ca^{2+} concentrations ($[Ca^{2+}]_i$; Nakajima et al., 2000). But, ursodeoxycholic acid at concentrations below 300 μM did not significantly increase $[Ca^{2+}]_i$ (Chisaki et al., 2001). Therefore, it also seems unlikely that $[Ca^{2+}]_i$ is involved in the inhibitory effects of ursodeoxycholic acid on endothelin-1 production.

It has been reported that nitric oxide reduces endothelin-1 production in endothelial cells mediated by cGMP-dependent pathway (Cao et al., 1994; Mitsutomi et al., 1999). Bile acids such as chenodeoxycholic acid increase nitric oxide production in HUVECs by increasing $[Ca^{2+}]_i$ (Nakajima et al., 2000). In the present study, ursodeoxycholic acid at concentrations higher than 300 μM increased nitric oxide production without significant changes in eNOS mRNA expression (Fig. 4). High concentrations of ursodeoxycholic acid increase $[Ca^{2+}]_i$ (Chisaki et al., 2001), which may be involved in ursodeoxycholic acid-induced nitric oxide increase. But the inhibitory effects of ursodeoxycholic acid on endothelin-1 were observed at the lower concentration, suggesting that the basic mechanism underlying these effects is different. In addition, tauroursodeoxycholic and glycoursodeoxycholic acids as well as ursodeoxycholic acid increased nitric oxide production in a similar manner, while the effects of these conjugates on endothelin-1 were less potent than those of ursodeoxycholic acid. Furthermore, to investigate the role of nitric oxide on ursodeoxycholic acid actions, the effects of L-NAME were investigated. L-NAME significantly inhibited the production of nitric oxide but failed to suppress the inhibitory effects of ursodeoxycholic acid on endothelin-1 production. These findings suggest that ursodeoxycholic acid inhibits endothelin-1 production in HUVECs via nitric oxide-independent mechanism.

In endothelial cells and aortic smooth muscle cells, the half-life of endothelin-1 mRNA is very short (approximately 20 min; Horie et al., 1991; Marsden and Brenner, 1992; Hu et al., 1992). This short lifespan of mRNA has been attributed to the presence of three AUUA sequence in the 3′ -untransated region that is thought to mediate selective mRNA (Inoue et al., 1989). Endothelin-1 mRNA is short lived and endothelin-1 is not stored in secretary granule, suggesting that endothelin-1 biosynthesis is mainly regulated at the levels of transcription (Rubanyi and Polokoff, 1994). Therefore, it is likely that the inhibitory effects of ursodeoxycholic acid on endothelin-1 production are due to the inhibition of the transcriptional level. In fact, the present study clearly showed that ursodeoxycholic acid significantly inhibited endothelin-1 mRNA expression.

The inhibitory effects of ursodeoxycholic acid on endothelin-1 production were observed at concentrations above 30 μM in the present study, and the significant inhibition was evident at 100 μM. The serum ursodeoxycholic acid concentration in patients with primary biliary cirrhosis receiving ursodeoxycholic acid therapy has been reported to vary between 10 and 100 μM (Stiehl et al., 1990; Kita et al., 1999), and it reached to approximately 50–100 μM in patients with liver cirrhosis, receiving ursodeoxycholic acid therapy (Chisaki et al., 2001), suggesting that physiological concentrations of ursodeoxycholic acid inhibit endothelin-1 production in human endothelial cells.

Endothelin-1 has been proposed to be involved in augmenting intrahepatic vascular resistance and subsequently contributing to portal hypertension in patients with hepatobiliary diseases (Rockey and Weisiger, 1996; Sogni et al., 1998; Reichen et al., 1998; Shah, 2001). Taken into account that hepatic endothelin-1 is derived from sinusoidal endothelial and stellate cells and modulates an intrahepatic vascular resistance in a paracrine or autocrine manner, endothelin-1 overproduction in the injured liver may increase portal pressure. Actually, endogenous endothelin-1 increases portal pressure in vivo as well as isolated perfused liver (Isales et al., 1993). A number of studies showed that plasma and hepatic endothelin-1 concentration were elevated in human and experimental liver cirrhosis and obstructive jaundice (Moller et al., 1995; Bernardi et al., 1996; Bruno et al., 2000). Thus, it is very likely that endothelin-1 may play a key role in various pathophysiological conditions such as cirrhotic portal hypertension. It has been reported that endothelin-1 receptor antagonists decrease portal pressure in the experimental cirrhotic rat (Rockey and Weisiger, 1996; Sogni et al., 1998; Reichen et al., 1998). Our findings showing that ursodeoxycholic acid inhibits production of endothelin-1 in human endothelial cells suggest that ursodeoxycholic acid therapy may prevent the development of several pathogenesis such as portal hypertension observed in patients with cirrhosis. In fact, ursodeoxycholic acid has

been reported to limit liver histological and portal hypertension induced by bile duct ligation in the rat (Poo et al., 1992). In addition, the increased circulating plasma endothelin-1 also contributes in part to renal dysfunction in patients with cirrhosis (Tsai et al., 1995), suggesting that ursodeoxycholic acid may provide the additional protective effects by inhibiting endothelin-1 production.

In conclusion, the present study provides novel evidence that ursodeoxycholic acid inhibits endothelin-1 production in human endothelial cells, but nitric oxide is not responsible for ursodeoxycholic acid effects on endothelin-1. Ursodeoxycholic acid therapy may prevent the development of several pathogenesis such as portal hypertension observed in patients with cirrhosis due to the improvement of endothelial function.

References

Alam, I., Bass, N.M., Bacchetti, P., Gee, L., Rockey, D.C., 2000. Hepatic tissue endothelin-1 levels in chronic liver disease correlate with disease severity and ascites. Am. J. Gastroenterol. 95, 199–203.

Bernardi, M., Gulberg, V., Colantoni, A., Trevisani, F., Gasbarrini, A., Gerbes, A.L., 1996. Plasma endothelin-1 and -3 in cirrhosis: relationship with systemic hemodynamics, renal function and neurohumoral systems. J. Hepatol. 24, 161–168.

Bruno, C.M., Neri, S., Sciacca, C., Caruso, L., 2000. Plasma endothelin-1 levels in liver cirrhosis. Int. J. Clin. Lab. Res. 30, 169–172.

Cao, W.B., Zeng, Z.P., Zhu, Y.J., Luo, W.C., Cai, B.Q., 1994. Inhibition of nitric oxide synthesis increases the secretion of endothelin-1 in vivo and in cultured endothelial cells. Chin. Med. J. (Engl.) 107, 822–826.

Chisaki, K., Nakajima, T., Iwasawa, K., Iida, H., Matsumoto, A., Tada, M., Komatsu, Y., Hirose, K., Miyamoto, K., Okuda, Y., Shiratori, Y., Goto, A., Hirata, Y., Nagai, R., Omata, M., 2001. Enhancement of endothelial nitric oxide production by chenodeoxycholic acids in patients with hepatobiliary diseases. Jpn. Heart J. 42, 339–353.

Cirillo, N.W., Zwas, R.F., 1994. Ursodeoxycholic acid in the treatment of chronic liver disease. Am. J. Gastroenterol. 89, 1447–1452.

Fiorucci, S., Antonelli, E., Morelli, O., Mencarelli, A., Casini, A., Mello, T., Palazzetti, B., Tallet, D., del Soldato, P., Morelli, A., 2001. NCX-1000, a NO-releasing derivative of ursodeoxycholic acid, selectively delivers NO to the liver and protects against development of portal hypertension. Proc. Natl. Acad. Sci. U. S. A. 98, 8897–8902.

Gandhi, C.R., Stephenson, K., Olson, M.S., 1990. Endothelin, a potent peptide agonist in the liver. J. Biol. Chem. 265, 17432–17435.

Garner, C.M., Mills, C.O., Elias, E., Neuberger, J.M., 1991. The effect of bile salts on human vascular endothelial cells. Biochim. Biophys. Acta 1091, 41–45.

Horie, M., Uchida, S., Yanagisawa, M., Matsushita, Y., Kurokawa, K., Ogata, E., 1991. Mechanisms of endothelin-1 mRNA and peptides induction by TGF-beta and TPA in MDCK cells. J. Cardiovasc. Pharmacol. 17 (Suppl. 7), S222–S225.

Hu, R.M., Levin, E.R., Pedram, A., Frank, H.J., 1992. Atrial natriuretic peptide inhibits the production and secretion of endothelin from cultured endothelial cells. Mediation through the C-receptor. J. Biol. Chem. 267, 17384–17389.

Inoue, A., Yanagisawa, M., Takuwa, Y., Mitsui, Y., Kobayashi, M., Masaki, T., 1989. The human preproendothelin-1 gene. Complete nucleotide sequence and regulation of expression. J. Biol. Chem. 264, 14954–14959.

Isales, C.M., Nathanson, M.H., Bruck, R., 1993. Endothelin-1 induces cholestasis which is mediated by an increase in portal pressure. Biochem. Biophys. Res. Commun. 191, 1244–1251.

Jo, T., Nagata, T., Iida, H., Imuta, H., Iwasawa, K., Ma, J., Hara, K., Omata, M., Nagai, R., Takizawa, H., Nagase, T., Nakajima, T., 2004. Voltage-gated sodium channel expressed in cultured human smooth muscle cells: involvement of SCN9A. FEBS Lett. 567, 339–343.

Kita, Y., Sakakura, H., Hirata, M., Harihara, Y., Tanaka, H., Ito, M., Yoshino, H., Takayama, T., Kubota, K., Hashizume, K., Makuuchi, M., 1999. Ursodeoxycholic acid in serum and liver tissue in patients with end-stage cholestatic liver cirrhosis. Transplant. Proc. 31, 2897–2898.

Kuddus, R.H., Nalesnik, M.A., Subbotin, V.M., Rao, A.S., Gandhi, G.R., 2000. Enhanced synthesis and reduced metabolism of endothelin-1 (ET-1) by hepatocytes—an important mechanism of increased endogeneous levels of ET-1 in liver cirrhosis. J. Hepatol. 33, 725–732.

Leivas, A., Jimenez, W., Lamas, S., Bosch-Marce, M., Oriola, J., Claria, J., Arroyo, V., Rivera, F., Rodes, J., 1995. Endothelin-1 does not play a major role in the homeostasis of arterial pressure in cirrhotic rats with ascites. Gastroenterology 108, 1842–1848.

Luketic, V.A., Sanyal, A.J., 1994. The current status of ursodeoxycholate in the treatment of chronic cholestatic liver disease. Gastroenterologist 2, 74–79.

Ma, J., Nakajima, T., Iida, H., Iwasawa, K., Terasawa, K., Oonuma, H., Jo, T., Morita, T., Imuta, H., Suzuki, J., Hirose, K., Okuda, Y., Yamada, N., Nagai, R., Omata, M., 2003. Inhibitory effects of ursodeoxycholic acid on the induction of nitric oxide synthase in vascular smooth muscle cells. Eur. J. Pharmacol. 464, 79–86.

Makino, I., Tanaka, H., 1998. From a choleretic to an immunomodulator: historical review of ursodeoxycholic acid as a medicament. J. Gastroenterol. Hepatol. 13, 659–664.

Marsden, P.A., Brenner, B.M., 1992. Transcriptional regulation of the endothelin-1 gene by TNF-α. Am. J. Physiol. 262, C854–C861.

Mitsutomi, N., Akashi, C., Odagiri, J., Matsumura, Y., 1999. Effects of endogeneous and exogeneous nitric oxide on endothelin-1 production in cultured vascular endothelial cells. Eur. J. Pharmacol. 364, 65–73.

Mitsuyoshi, H., Nakasima, T., Sumida, Y., Yoh, T., Nakajima, Y., Ishikawa, H., Inaba, K., Sakamoto, Y., Okanoue, T., Kashima, K., 1999. Ursodeoxycholic acid protects hepatopcytes against oxidative injury via induction of antioxidants. Biochem. Biophys. Res. Commun. 24, 537–542.

Moller, S., Gulberg, V., Henriksen, J.H., Gerbes, A.L., 1995. Endothelin-1 and endothelin-3 in cirrhosis: relations to systemic and splanchnic haemodynamics. J. Hepatol. 23, 135–144.

Moncada, S., Palmer, R.M., Higgs, E.A., 1991. Nitric oxide: physiology, pathophysiology, and pharmacology. Pharmacol. Rev. 43, 109–142.

Nakajima, T., Okuda, Y., Chisaki, K., Shin, W.S., Iwasawa, K., Morita, T., Matsumoto, A., Suzuki, J.I., Suzuki, S., Yamada, N., Toyo-oka, T., Nagai, R., Omata, M., 2000. Bile acids increase intracellular Ca^{2+} concentration and nitric oxide production in vascular endothelial cells. Br. J. Pharmacol. 130, 1457–1467.

Nathan, C., 1992. Nitric oxide as a secretory product of mammalian cells. FASEB J. 6, 3051–3064.

Pinzani, M., Milani, S., De Franco, R., Grappone, C., Caligiuri, A., Gentilini, A., Tosti-Guerra, C., Maggi, M., Failli, P., Ruocco, C., Gentilini, P., 1996. Endothelin-1 is overexpressed in human cirrhotic liver and exerts multiple effects on activated hepatic stellate cells. Gastroenterology 110, 534–548.

Poo, J.L., Feldmann, G., Erlinger, S., Braillon, A., Gaudin, C., Dumont, M., Lebrec, D., 1992. Ursodeoxycholic acid limits liver histologic alterations and portal hypertension induced by bile duct ligation in the rat. Gastroenterology 102, 1752–1759.

Poo, J.L., Estanes, A., Pedraza-Chaverri, J., Cruz, C., Uribe, M., 1995. Effects of ursodeoxycholic acid on hemodynamic and renal function abnormalities induced by obstructive jaundice in rats. Ren. Fail. 17, 13–20.

Reichen, J., Gerbes, A.L., Steiner, M.J., Sagesser, H., Clozel, M., 1998. The effect of endothelin and its antagonist Bosentan on hemodynamics and microvascular exchange in cirrhotic rat liver. J. Hepatol. 28, 1020–1030.

Rockey, D.C., Weisiger, R.A., 1996. Endothelin induced contractility of stellate cells from normal and cirrhotic rat liver: implications for regulation of portal pressure and resistance. Hepatology 24, 233–240.

Rockey, D.C., Fouassier, L., Chung, J.J., Carayon, A., Vallee, P., Rey, C., Housset, C., 1998. Cellular localization of endothelin-1 and increased production in liver injury in the rat: potential for autocrine and paracrine effects on stellate cells. Hepatology 27, 472–480.

Rubanyi, G.M., Polokoff, M.A., 1994. Endothelins: molecular biology, biochemistry, pharmacology, physiology, and pathophysiology. Pharmacol. Rev. 46, 325–415.

Serradeil-Le Gal, C., Jouneaux, C., Sanchez-Bueno, A., Raufaste, D., Roche, B., Preaux, A.M., Maffrand, J.P., Cobbold, P.H., Hanoune, J., Lotersztajin, S., 1991. Endothelin action in rat liver. Receptors, free Ca^{2+} oscillation, and activation of glycogenolysis. J. Clin. Invest. 87, 133–138.

Shah, V., 2001. Cellular and molecular basis of portal hypertension. Clin. Liver Dis. 5, 629–644.

Sogni, P., Moreau, R., Gomola, A., Cadano, A., Cailmail, S., Calmus, Y., Clozel, M., Lebrec, D., 1998. Beneficial hemodynamic effects of bosentan, a mixed ETA and ETB receptor antagonist, in portal hypertensive rats. Hepatology 28, 655–659.

Stiehl, A., Rudolph, G., Raedsch, R., Moller, B., Hopf, U., Lotterer, E., Bircher, J., Folsch, U., Klaus, J., Endele, R., 1990. Ursodeoxycholic acid-induced changes of plasma and urinary bile acids in patients with primary biliary cirrhosis. Hepatology 12, 492–497.

Tieche, S., De Gottardi, A., Kappeler, A., Shaw, S., Sagesser, H., Zimmermann, A., Reichen, J., 2001. Overexpression of endothelin-1 in bile duct ligated rats: correlation with activation of hepatic stellate cells and portal pressure. J. Hepatol. 34, 38–45.

Tsai, Y.T., Lin, H.C., Yang, M.C., Lee, F.Y., Hou, M.C., Chen, L.S., Lee, S.D., 1995. Plasma endothelin levels in patients with cirrhosis and their relationships to the severity of cirrhosis and renal function. J. Hepatol. 23, 681–688.

Yanagisawa, M., Kurihara, H., Kimura, S., Tomobe, Y., Kobayashi, M., Mitsui, Y., Yazaki, Y., Goto, K., Masaki, T., 1988. A novel potent vasoconstrictor peptide produced by vascular endothelial cells. Nature 332, 411–415.

Gene Therapy (2004) 11, 1370–1377

www.nature.com/gt

RESEARCH ARTICLE

Expansion of genetically corrected neutrophils in chronic granulomatous disease mice by cotransferring a therapeutic gene and a selective amplifier gene

T Hara[1,2], A Kume[1], Y Hanazono[3], H Mizukami[1], T Okada[1], H Tsurumi[2], H Moriwaki[2], Y Ueda[4], M Hasegawa[4] and K Ozawa[1,5]

[1]*Division of Genetic Therapeutics, Center for Molecular Medicine, Jichi Medical School, Tochigi, Japan;* [2]*First Department of Internal Medicine, Gifu University School of Medicine, Gifu, Japan;* [3]*Division of Regenerative Medicine, Center for Molecular Medicine, Jichi Medical School, Tochigi, Japan;* [4]*DNAVEC Research Inc., Ibaraki, Japan; and* [5]*Division of Hematology, Department of Medicine, Jichi Medical School, Tochigi, Japan*

Hematopoietic stem cell gene therapy has not provided clinical success in disorders such as chronic granulomatous disease (CGD), where genetically corrected cells do not show a selective advantage in vivo. To facilitate selective expansion of transduced cells, we have developed a fusion receptor system that confers drug-induced proliferation. Here, a 'selective amplifier gene (SAG)' encodes a chimeric receptor (GcRER) that generates a mitotic signal in response to estrogen. We evaluated the in vivo efficacy of SAG-mediated cell expansion in a mouse disease model of X-linked CGD (X-CGD) that is deficient in the NADPH oxidase gp91^{phox} subunit. Bone marrow cells from X-CGD mice were transduced with a bicistronic retrovirus encoding GcRER and gp91^{phox}, and transplanted to lethally irradiated X-CGD recipients. Estrogen was administered to a cohort of the transplants, and neutrophil superoxide production was monitored. A significant increase in oxidase-positive cells was observed in the estrogen-treated mice, and repeated estrogen administration maintained the elevation of transduced cells for 20 weeks. In addition, oxidase-positive neutrophils were increased in the X-CGD transplants given the first estrogen even at 9 months post-transplantation. These results showed that the SAG system would enhance the therapeutic effects by boosting genetically modified, functionally corrected cells in vivo.
Gene Therapy (2004) **11**, 1370–1377. doi:10.1038/sj.gt.3302317; Published online 1 July 2004

Keywords: *chronic granulomatous disease; selective amplifier gene; respiratory burst; estrogen-binding domain*

Introduction

Gene transfer to hematopoietic stem cells (HSCs) holds promise to provide a long-standing cure of many lymphohematological diseases. One of the candidate disorders is chronic granulomatous disease (CGD), a rare inherited phagocyte dysfunction that renders patients particularly susceptible to catalase-positive microorganisms.[1] The disease is caused by a defect in microbicidal oxidant production, resulting from mutations in the genes encoding four essential subunits of the phagocyte NADPH oxidase (*phox*). The X-linked form of CGD (X-CGD), accounting for about 70% of all cases, is due to genetic mutations in the large subunit of the oxidase cytochrome b_{558}, which is a 91 kDa glycoprotein referred to as gp91^{phox}.[2] A rare autosomal recessive form of CGD results from a defect in the gene encoding p22^{phox}, the small subunit of the cytochrome (about 5%). Other patients have an autosomal recessive trait with a deficiency of either p47^{phox} (20–25%) or p67^{phox} (<5%), which are two soluble proteins in the oxidase complex.

Correspondence: Dr A Kume or Dr K Ozawa, Division of Genetic Therapeutics, Center for Molecular Medicine, Jichi Medical School, 3311-1 Yakushiji, Minamikawachi, Tochigi 329-0498, Japan
Received 7 October 2003; accepted 3 February 2004; published online 1 July 2004

Although prophylactic antibiotics and interferon γ constitute a cornerstone of CGD management and have brought about a better outlook,[3,4] morbidity caused by infection or granulomatous complications remains significant. Allogeneic bone marrow transplantation (BMT) has not been well adopted because of procedure-associated risks and difficulty in finding a suitable donor, but this therapeutic option is increasingly considered for young patients with histocompatible siblings.[5] Recently, a study of patients who underwent nonmyeloablative stem cell transplantation was published, with a better outcome with young patients as well.[6]

Somatic gene therapy targeted at autologous HSCs can bypass problems involved in allotransplantation such as acute graft rejection and graft-versus-host disease.[7] For CGD, correction of only a minority of phagocytes is likely to provide clinical benefit, because a partial chimerism after BMT has freed patients from severe infections and female carriers of X-CGD with as few as 5–10% oxidase-positive neutrophils are often asymptomatic.[8–10] Likewise, preclinical studies with mouse models have provided a rationale for this approach.[11–14] So far, a few phase I clinical gene therapy trials have been conducted, but the percentages of corrected neutrophils have been too low to impact the disease phenotype.[15]

A potential transgene-induced immune reaction remains to be discussed extensively, but maintenance of low-level chimerism in some transplants suggests that rejection by this mechanism is less likely to occur.

Even with the recent refinement of transduction protocols, transducing enough human HSCs is a major challenge to gene therapy for inherited and acquired blood cell disorders.[16] Thus, it is desirable to expand genetically corrected cells in the body, to improve the therapeutic efficacy of stem cell gene therapy. One strategy to achieve this goal is to help their preferential outgrowth through drug selection. On transduction of the target cells with a therapeutic gene and a drug-resistance gene, administering the corresponding cytotoxic drug leads to an increase of genetically modified cells.[17,18] An alternative approach is to confer a direct proliferative advantage on the genetically modified cells, provided that the mitogenic stimulation is restricted to the genetically modified cells in a controllable manner.[19,20]

We have developed a novel system for the selective expansion of transduced cells to compensate for the low frequency of genetically corrected cells.[21–23] The expansion system comprises a fusion protein and a stimulator drug. As a growth signal generator, a chimeric receptor (GcRER) was constructed with the granulocyte colony-stimulating factor (G-CSF) receptor (GcR) and the hormone-binding domain of the estrogen receptor (ER-HBD). The artificial gene encoding the fusion protein was referred to as a 'selective amplifier gene (SAG)'. We showed that transduced hematopoietic stem/progenitor cells were expandable with this system in murine and primate models.[24,25] In the present study, a bicistronic retroviral vector carrying the human gp91^{phox} (hgp91) gene and a modified SAG was evaluated in a mouse model of X-CGD.

Results

Retroviral vector carrying the gp91^{phox} gene and a selective amplifier gene

Figure 1a shows the structure of fusion proteins comprising GcR and ER-HBD. The prototype SAG encodes a fusion protein made up of the full-length mouse GcR and the rat ER-HBD.[21] In ΔGcRER, the G-CSF binding domain (amino acids 5–195 in the full-length GcR) was deleted to free it from the endogenous G-CSF.[21] In addition, the most proximal cytoplasmic tyrosine (position 703) of the mouse GcR was replaced with phenylalanine in ΔY703FGcRER to attenuate the differentiation signal, based on the result that the tyrosine residue was strongly involved in granulocyte maturation.[22]

Figure 1b shows the structure of the retroviral vector used in this study. The vector, MGK/h91GE, was constructed with MFG and MSCV backbones,[26,27] the hgp91 gene and the picornavirus-derived internal ribosome entry site (IRES)-linked ΔY703FGcRER gene.[28] Ecotropic BOSC23 packaging cells were transfected with the MGK/h91GE vector plasmid and the viral supernatant was harvested.[29] Viral titer of the supernatant was estimated to be 5×10^5 particles/ml, by a simplified RNA dot blot protocol along with the plasmid as a reference.[30] Ba/F3 cells and gp91^{phox}-deficient PLB-985 myeloid cells

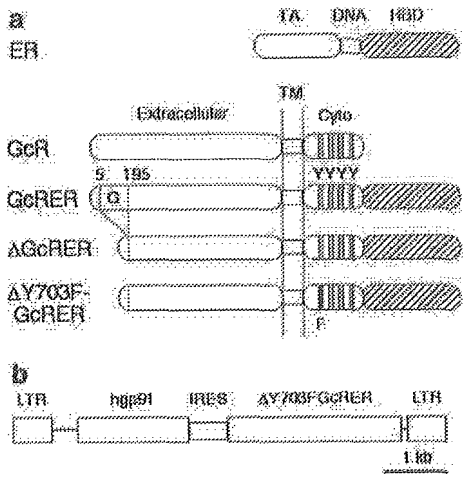

Figure 1 Structure of selective amplifier gene-encoded proteins and gene transfer vector. (a) GcRER is a fusion protein comprising the full-length mouse G-CSF receptor (GcR) and the hormone-binding domain of the rat estrogen receptor (ER). ΔGcRER is deleted of the G-CSF binding domain of GcR (amino acids 5–195). ΔY703FGcRER has a substitution of phenylalanine for tyrosine 703 in GcR. TA, transactivating domain; DNA, DNA-binding domain; HBD, hormone-binding domain; Extracellular, extracellular domain; TM, transmembrane domain; Cyto, cytoplasmic domain; G, G-CSF binding domain; Y, tyrosine residue; F, phenylalanine substitution for Y703. (b) Schematic representation of bicistronic vector (MGK/h91GE) carrying the human gp91^{phox} gene and a selective amplifier gene. LTR, long-terminal repeat; hgp91, human gp91^{phox} gene; IRES, internal ribosome entry site.

were transduced with the viral supernatant, and the expression of the vector-encoded hgp91 was confirmed by fluorescence-activated cell sorting (FACS) with 7D5 monoclonal antibody (a gift from Dr M Nakamura, Nagasaki University, Nagasaki, Japan; FACS data not shown).[31,32]

Transduction of X-CGD progenitors

The efficiency of the MGK/h91GE vector was evaluated by transducing X-CGD mouse bone marrow (BM) cells. The X-CGD mouse was created by targeted disruption of the X-linked gp91^{phox} gene, and its phagocytes are devoid of respiratory burst activity.[11] As a result, these mice share many characteristics of the human CGD phenotype, including an elevated susceptibility to *Aspergillus* species. The mice were backcrossed to C57BL/6; subsequently, the X-CGD allele was introduced into the Ly5.1-C57BL/6 congenic background to allow Ly5.1/5.2 chimerism to be analyzed in the BM transplants.

We assessed the *in vitro* responsiveness of vector-transduced cells to estrogen using a clonogenic progenitor assay. BM cells were harvested from male Ly5.1-X-CGD mice treated with intraperitoneal 5-fluorouracil (5-FU) 2 days before. Following prestimulation with stem cell factor (SCF) and interleukin-6 (IL-6) for 2 days, a major part of BM cells was transduced with the MGK/h91GE viral supernatant according to a standard fibronectin-assisted protocol.[33] The remainder part was incubated in the same culture condition as the prestimulation for another 2 days, instead of being transduced with the viral supernatant ('untransduced cells'). Then, untransduced cells and an aliquot of transduced cells were subjected to methylcellulose culture with a cytokine

Table 1 Clonogenic progenitor assay

Growth factors	*Total colony number (% NBT-positive)*	
	Transduced BM	*Untransduced BM*
None	0 (ND)	0 (ND)
IL-3+SCF+G-CSF+Epo	524 (29%)	547 (0%)
E_2	228 (96%)	0 (ND)

Transduced and untransduced X-CGD mouse bone marrow (BM) cells were inoculated onto methylcellulose in duplicate (1×10^5 cells/dish). Colonies were counted at day 10, and an *in situ* NBT test was carried out to detect superoxide production by individual colonies. NBT, nitroblue tetrazolium; ND, not done; IL-3, mouse interleukin-3; SCF, rat stem cell factor; G-CSF, human granulocyte colony-stimulating factor; Epo, human erythropoietin; E_2, estradiol.

combination (SCF, IL-3, erythropoietin (Epo) and G-CSF), 10^{-7} M 17β-estradiol (E_2) alone, or no stimulation. The E_2 concentration that supported optimal growth of the GcRER-transduced murine progenitors was chosen.[21,23] Table 1 summarizes the result of the colony assay at 10 days of growth. No colony was observed in the culture without stimulation, regardless of whether the cells were transduced or untransduced. With the cytokine cocktail, both transduced and untransduced X-CGD BM cells yielded comparable number of colonies (about 500 colonies out of 2×10^5 cells). Most of them were myeloid, and there were a few erythroid and mixed colonies. Thus, transduction with MGK/h91GE did not show positive or negative effect on cytokine-induced colony formation. Finally, the untransduced BM formed no colony in the presence of E_2 alone, as we observed previously.[21,23] In contrast, 10^{-7} M E_2 induced about 200 colonies from 2×10^5 transduced X-CGD BM cells, most of which were granulocyte/monocyte colonies. Considering the very low background colony formation in this assay, these E_2-induced colonies must be derived from vector-transduced progenitors that actually expressed SAG. From the ratio of E_2-induced colonies to cytokine-induced colonies, the *ex vivo* transduction efficiency was estimated to be 44%.

On day 10 of the methylcellulose culture, the colonies were subjected to an *in situ* nitroblue tetrazolium (NBT) test to detect respiratory burst activity. In this assay, most phorbol myristate acetate (PMA)-stimulated wild-type (WT) granulocyte colonies reduced NBT and turned blue (not shown), while the cytokine-induced colonies derived from untransduced X-CGD BM showed no respiratory burst activity (Table 1). As for MGK/h91GE-transduced X-CGD BM, 29% of the cytokine-induced colonies were NBT-positive, while nearly all of the E_2-induced colonies showed a respiratory burst (Table 1 and Figure 2). These results indicated that the SAG/estrogen system selectively expanded genetically modified progenitors *in vitro*, and the estrogen-induced colonies actually coexpressed ΔY703FGcRER and $gp91^{phox}$. NBT positivity in the cytokine-induced colonies (29%) would represent functional transduction efficiency based on $gp91^{phox}$ expression (see Discussion).

In vivo expansion of functionally corrected neutrophils

In parallel with the *in vitro* progenitor assay, the same batch of MGK/h91GE-transduced Ly5.1-X-CGD BM cells

Figure 2 *In situ colony NBT test. X-CGD bone marrow cells were transduced with MGK/h91GE vector and 2×10^5 cells were subjected to methylcellulose culture with 10^{-7} M estradiol. On day 10, the colonies were overlaid with RPMI medium containing NBT and PMA. Nearly all the estrogen-induced colonies were NBT-positive with blue formazan precipitates.*

was transplanted to lethally irradiated male Ly5.2-X-CGD recipients ($n = 8$). Donor-derived Ly5.1 cells rapidly repopulated in the recipients; a series of FACS analysis revealed that the overall white blood cell (WBC) chimerism was 81–91% at 4 weeks post-BMT, and remained above 90% thereafter (FACS data not shown). Following hematopoietic reconstitution, the frequency of oxidase-positive granulocytes in the peripheral blood was monitored by flow cytometry. Leukocytes were loaded with dihydrorhodamine 123 (DHR) and stimulated with PMA.[34] Figure 3 shows representative FACS data of this assay; most PMA-stimulated granulocytes ($Gr1^{high}$) from a WT C57BL/6 mouse produced superoxide to reduce DHR (Figure 3a and e), while granulocytes from an untreated X-CGD mouse did not (Figure 3b and f).

At 6 weeks post-BMT, when the percentage of DHR-positive neutrophils in the transplants was $9.6 \pm 3.2\%$ (range 7.0–17.0%), four out of eight animals were given E_2 intraperitoneally to address whether the drug would induce an expansion of functionally corrected neutrophils. Our preliminary study showed that about 1 mg of E_2 per mouse (ca. 25 g body weight) was required to achieve a serum estrogen level above 10^{-7} M 24 h after injection (unpublished). Based on this observation, the animals were given 1 mg of E_2 in two doses for 3 days, to ensure trough E_2 levels above 10^{-7} M. This treatment was repeated six times with 4-week intervals until 26 weeks post-BMT.

At 2 weeks after the first course of E_2, three out of four challenged mice had increased levels of DHR-positive neutrophils (from 8.3–17.0 to 12.9–67.3%), while one animal had a lowered DHR positivity (from 9.7 to 5.0%). Figure 3c and g shows an E_2-treated mouse that exhibited the most prominent expansion of oxidase-positive neutrophils. In this animal, oxidase-positive granulocytes were increased from 17.0 to 67.3% (Figure 3g). On the other hand, frequencies of DHR-positive granulocytes in the unstimulated mice were unchanged or

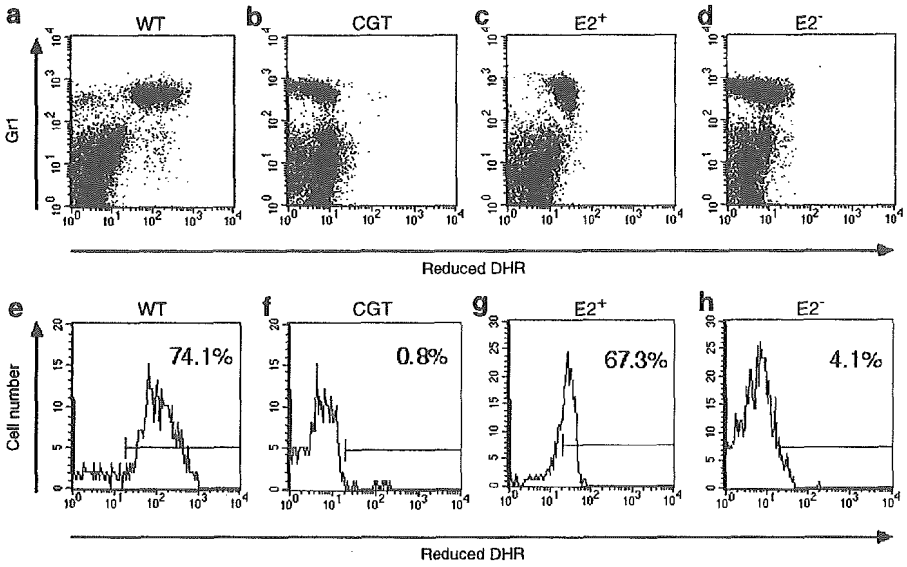

Figure 3 Flow cytometry of DHR assay. Mouse peripheral blood was stimulated with PMA, incubated with DHR and stained with Gr1-PE/Cy5. In the dot plots (a–d), the X-axis represents DHR reduced by superoxide, and the Y-axis represents expression of a granulocyte differentiation marker Gr1. In the histograms (e–h), $Gr1^{high}$-gated cells were shown to highlight superoxide formation by neutrophils. (a and e) A wild-type C57BL/6 mouse (WT). (b and f) An untreated X-CGD mouse (CGD). (c and g) An X-CGD transplant 2 weeks after the first estrogen administration (E_2^+). (d and h) An X-CGD transplant not administered estrogen (E_2^-).

lowered. Only 1.7–10.1% (4.3±3.9%) of neutrophils produced superoxide, and Figure 3d and h shows a FACS analysis of an unstimulated animal. A parallel NBT slide test showed comparable frequencies of oxidase-positive cells in these mice (NBT slides not shown).

Although the initial response to estrogen varied among transplants, repeated E_2 administration led to an increase in respiratory burst-positive neutrophils in these animals. As shown in Figure 4a, the frequency of DHR-positive neutrophils at 16 weeks post-BMT (2 weeks after the third E_2 administration) was elevated in all the treated animals compared to that seen before the drug challenge (from 11.0±4.0 to 35.7±9.1%), and the increase was significant ($P=0.014$ by paired t-test). The absolute number of oxidase-positive neutrophils was also significantly increased, as shown in Figure 4b (from 244±211 to 486±302/μl; $P=0.019$ by paired t-test).

Prolonged increase in oxidase-positive neutrophils

With repeated E_2 administration, the drug-treated X-CGD transplants maintained a higher level of genetically corrected neutrophils than the untreated animals. A difference between groups was observed 2 weeks after the initial treatment; the drug-treated animals (Group 1) showed higher percentages of DHR-positive neutrophils (27.5±27.8%) than the untreated mice (Group 2; 4.3±3.9%) as shown in Figure 5a ($P=0.043$ by Mann–Whitney U-test). This figure also shows that the levels of oxidase-positive granulocytes were significantly higher in Group 1 than Group 2 at most time points during the repeated course of E_2 administration (asterisks in Figure 5a, $P<0.05$ by Mann–Whitney U-test). The absolute number of oxidase-positive cells was higher in Group 1 than Group 2 on E_2 treatment as well (asterisks in Figure 5b, $P<0.05$ by Mann–Whitney U-test).

At a later time point (38 weeks post-BMT), the treatment was switched. That is, the mice in Group 2

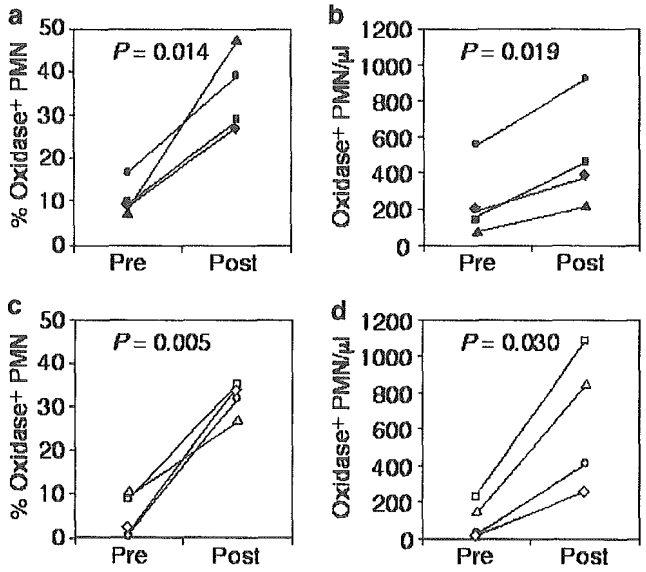

Figure 4 Comparison of oxidase-positive granulocytes before and after estrogen administration. Frequencies (a and c) and absolute numbers (b and d) of oxidase-positive polymorphonuclear leukocytes (PMN) from individual X-CGD transplants are shown. (a and b) Oxidase-positive PMN in Group 1 mice before estrogen administration (Pre; 6 weeks post-BMT) and after the third estrogen injection (Post; 16 weeks post-BMT). The increase was significant by paired t-test (a, $P=0.014$; b, $P=0.019$). (c and d) Oxidase-positive PMN in Group 2 mice before estrogen administration (Pre; 38 weeks post-BMT) and after estrogen injection (Post; 40 weeks post-BMT) at a later time point. The increase was significant by paired t-test (c, $P=0.005$; d, $P=0.030$). Each animal is represented by a different symbol to track the frequency and number of oxidase-positive PMN.

were given E_2 for 3 days, while the animals in Group 1 were left unchallenged. The E_2-stimulated animals showed a remarkable increase in DHR-positive cells. The percentage of DHR-positive granulocytes rose from

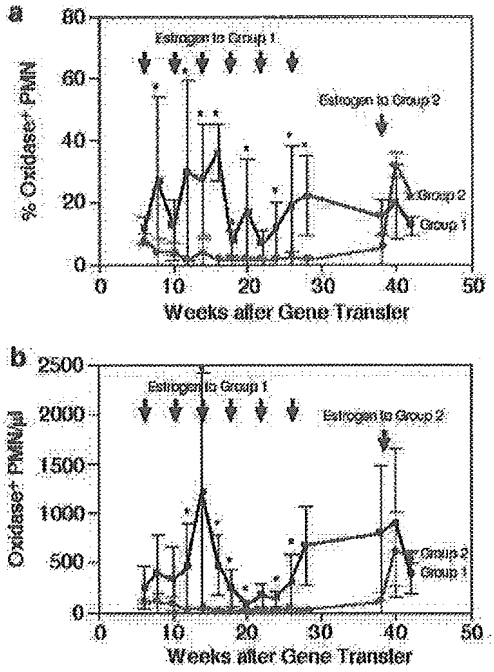

Figure 5 Estrogen-induced expansion of oxidase-positive granulocytes. Graphs indicate the time course of the change in frequency (a) and absolute number (b) of oxidase-positive granulocytes following exposure to estrogen. To mice in Group 1 ($n=4$), estrogen was given in six courses with 4-week intervals from 6 to 26 weeks post-BMT (black line). Mice in Group 2 ($n=4$) were given estrogen only once at 38 weeks post-BMT (gray line). Asterisks indicate time points when significantly more oxidase-positive cells existed in Group 1 than Group 2 ($P<0.05$ by Mann–Whitney U-test).

4.8 ± 4.7 to $31.7\pm3.8\%$ ($P=0.005$ by paired t-test, Figures 4c and 5a), and the absolute number increased from 96 ± 104 to $638\pm378/\mu l$ ($P=0.030$ by paired t-test, Figures 4d and 5b) in 2 weeks. This result indicated that transduced long-term repopulating cells were maintained in the animals and readily responsive to estrogen, thereby giving rise to an elevated level of corrected neutrophils on drug administration.

During the observation period, the administration of E_2 did not lead to any apparent hematological aberration in the treated mice; none of the recipients of transduced marrow have developed a proliferative disorder, regardless of whether E_2 was administered or not. Apparent feminization was not observed after the periodic estrogen administration in the transplanted male mice.

Discussion

In contrast to successful preclinical gene-transfer studies using mouse models,[13,14] the levels of corrected neutrophils have been too low to impact the CGD phenotype in phase I clinical trials like most gene-transfer attempts targeting human HSCs.[15] In contrast, Fischer and colleagues showed a significant T-lymphocyte reconstitution in a series of patients with X-linked severe combined immunodeficiency (X-SCID) following oncoretrovirus-mediated gene transfer.[35,36] This success largely owes to an extremely strong growth advantage of lymphocyte precursors transduced with a functional common γ chain (γc) gene.[37] However, an excessive growth stimulation may be harmful. Recently, a lymphoproliferative disorder occurred in patients treated in the X-SCID gene therapy following aberrant activation of *LMO2* oncogene by insertional mutagenesis.[38,39] In these patients, a strong and continuous mitogenic stimulation via functional γc may bring about additional events besides *LMO2* activation, finally leading to uncontrolled clonal proliferation. Therefore, for most HSC gene therapy candidate diseases in which a therapeutic gene *per se* does not confer a growth advantage, controlled expansion of transduced stem/progenitor cells is desirable.

For this purpose, we have developed selective amplifier genes,[21] and showed controllable *in vivo* expansion of marker gene-transduced hematopoietic cells in murine and primate models.[24,25] In the present study, we showed that functionally corrected cells were expandable using the SAG system in an actual disease model of CGD. An *in vitro* NBT assay showed that estrogen specifically induced functionally corrected colonies. It is currently unclear why gene transfer efficiency based on the total number of colonies (44%) differed from that based on NBT positivity (29%). At present, we consider the latter estimation (29% based on NBT positivity) as more accurate and reliable, because the former is based on an indirect calculation with colony number, which inherently includes fluctuation.

We also showed an *in vivo* expansion of corrected neutrophils. Following estrogen stimulation, the ratio and number of oxidase-positive granulocytes were elevated, and repeated drug administration maintained an increased level of corrected cells. Furthermore, superoxide-producing cells increased remarkably in the transplants given estrogen at a later time point (Group 2 in Figure 5), suggesting that transduced long-term repopulating cells remain responsive to estrogen and that on-demand expansion of functional neutrophils is feasible in CGD. As mentioned, we observed that the initial response to estrogen varied among transplants in Group 1, and the reason for this variation is yet to be clarified. Considering that the mice in Group 2 responded to E_2 with little deviation at a later time point, the early E_2 administration to Group 1 may account, in part, for this variation. The mice in Group 1 were given E_2 at 6 weeks post-BMT, when the donor-derived hematopoiesis might not have reached a steady state and varied among animals considerably.

Including the present study, we have not encountered a neoplastic outgrowth of SAG-transduced cells in the animals examined thus far, including a primate system.[24,25] Blau and colleagues have presented another conditional expansion system in which an FK506-binding protein 12-based fusion receptor is activated by a dimerizing crosslinker, and no cancerous event has been reported.[19,40,41] Still more extensive studies are required to clear safety issues concerning uncontrolled proliferation. We are carrying out serial transplantation of SAG-transduced BM in an attempt to predict whether such complications would arise in a longer-term follow-up. In addition, large animal studies with clinically relevant protocols are mandatory to address the safety and feasibility of regulated cell expansion in HSC gene therapy.

Materials and methods

Plasmid construction

To transduce X-CGD hematopoietic cells with the hgp91 gene and a modified SAG, a bicistronic retrovirus vector was constructed. The vector, MGK/h91GE, had a hybrid backbone (MGK) comprising the long-terminal repeats (LTRs) and the primer-binding site from MSCV and the *gag* through to the *env* initiation codon from MFG.[26,27,42] The 5′-half of hgp91 cDNA (from the initiation codon to the internal *AseI* site) was derived from pBS/hgp91,[31] by amplification with the polymerase chain reaction (PCR) (upstream primer, 5′-TCTGCCACCATGGGGAACT-3′, and downstream primer, 5′-GCAAGGCCAATGAA GAAGAT-3′) to create an *NcoI* site at the initiation codon. The 3′-half of hgp91 (from the internal *AseI* site to the stop codon) was PCR-amplified on pBS/hgp91 using an upstream primer, 5′-GGCATCACTGGAGTTGTCA-3′, and a downstream primer, 5′-GAGGATCCTTA GAAGTTTTCCTTGTTGAA-3′, to add a *Bam*HI site at the 3′ end. The fragments were cloned into the *Nco*I–*Bam*HI site of MGK by trimolecular ligation to yield MGK/hgp91.[42] The 5′ half of the SAG (from the initiation codon to the internal *Dra*III site) was PCR-amplified on pBS/ΔY703FGcRER,[22] with 5′-AAATGGGACCTCTGG GAGCCTGCACCCTG-3′ as an upstream primer and a *Dra*III site-linked downstream primer (5′-AGAA CAGCTGCACACTCACT-3′) to create a *Ppu*MI site at the initiation codon. The 3′ half of the SAG (from the *Dra*III site to the stop codon) was PCR-amplified on pBS/ ΔY703FGcRER with 5′-AAGGCCCCCACCATCAGA CT-3′ as an upstream primer and an *Xho*I site-linked downstream primer (5′-CTGGCTCGAGTCAGATGG TGTTGGGGAAG-3′) to add an *Xho*I site to the 3′ end. The fragments were cloned into the *Ppu*MI–*Xho*I site of pCGI,[43] which contains the encephalomyocarditis virus-derived IRES,[28] by trimolecular ligation. Subsequently, the IRES-ΔY703FGcRER cassette was obtained as a *Bam*HI–*Xho*I fragment, and inserted between the hgp91 and the 3′-LTR of MGK/hgp91, resulting in the final construct MGK/h91GE (Figure 1b).

Animals

Targeted disruption of the X-linked gp91^{phox} gene in the mouse was described.[11] The X-CGD mice backcrossed to Ly5.2-C57BL/6 were a gift from Dr MC Dinauer (Indiana University, Indianapolis, IN, USA). The X-CGD mice were crossed with Ly5.1-congenic C57BL/6 mice, and both Ly5.1- and Ly5.2-X-CGD mice were maintained under specific pathogen-free conditions. The animals were given free access to autoclaved food and ultraviolet-irradiated water and treated according to the institutional codes governing animal rights. WT Ly5.2-C57BL/6 mice were purchased from Clea Japan (Tokyo, Japan).

Retroviral transduction

Ecotropic retroviral supernatant was prepared by transient transfection of BOSC23 packaging cells (American Type Culture Collection CRL-11554, Manassas, VA, USA) with MGK/h91GE using Lipofectamine (Invitrogen, Grand Island, NY, USA), following the manufacturer's protocol.[29] X-CGD mouse BM cells were retrovirally transduced using a fibronectin-assisted protocol.[25,33] Male Ly 5.1-X-CGD mice were injected intraperitoneally with 150 mg/kg 5-FU (Kyowa Hakko, Tokyo, Japan), and BM cells were collected 2 days postinjection. Low-density mononuclear cells were separated using Lympholyte-M (Cedarlane Laboratories, Hornby, Canada) and stimulated for 2 days with α-Minimum Essential Medium (Invitrogen) containing 100 ng/ml recombinant rat SCF (provided by Amgen, Thousand Oaks, CA, USA) and 100 U/ml recombinant human IL-6 (provided by Ajinomoto, Kawasaki, Japan).[44] The cells were then incubated in the fresh viral supernatant on plates precoated with recombinant human fibronectin fragment CH-296 (RetroNectin; provided by Takara Bio, Otsu, Japan) for 2 days under the same conditions. Supernatant infection was repeated five times during transduction, and the manipulated cells were recovered using Cell Dissociation Buffer (Invitrogen). As a negative control, an aliquot of the prestimulated cells was incubated in α-Minimum Essential Medium containing SCF and IL-6 for another 2 days ('untransduced cells').

Clonogenic progenitor assay

Hematopoietic progenitors were assayed using StemPro Methylcellulose Medium (Invitrogen) supplemented with appropriate growth factors. Transduced and untransduced X-CGD mouse BM cells were seeded onto Petri dishes at a density of 1×10^5 cells/dish in 1 ml of StemPro medium containing either no growth factor, 10^{-7} M E_2 (Sigma, St Louis, MO, USA) alone, or a cytokine cocktail of 2 U/ml recombinant human Epo (provided by Chugai Pharmaceuticals, Tokyo, Japan), 100 ng/ml SCF, 20 ng/ml recombinant human G-CSF (provided by Chugai Pharmaceuticals) and 100 U/ml IL-3.[21–23] After 10 days of incubation, colonies were counted and assayed for respiratory burst activity using an *in situ* NBT test (NBT from Sigma).[45] A one-fifth volume of NBT-saturated RPMI-1640 medium (Invitrogen) containing 100 ng/ml PMA (Sigma) and 5% human serum albumin (Baxter Healthcare, Deerfield, IL, USA) was layered onto the methylcellulose culture and incubated at 37°C. After 1 h of incubation, the dishes were examined on an inverted microscope, and the colonies with blue formazan precipitates were scored as NBT-positive.

BMT and estrogen administration

For hematopoietic reconstitution with retrovirally transduced Ly5.1-X-CGD BM cells, 8–10-week-old male Ly5.2-X-CGD recipients were lethally irradiated (split dose of 11 Gy at an interval of 3 h with ^{137}Cs using Gammacell 40, Nordion International, Kanata, Canada) and transplanted with the transduced BM cells. A total of $2–3 \times 10^6$ cells per recipient were given by tail vein injection. WBCs were stained with a fluorescein isothiocyanate-conjugated anti-Ly5.2 antibody (Pharmingen, San Diego, CA) and a phycoerythrin (PE)-conjugated anti-Ly5.1 antibody (Pharmingen) to measure chimerism with a FACScan (Becton Dickinson, San Jose, CA, USA). After hematopoietic reconstitution, one half of the transplanted mice were administered with estrogen (Group 1). Starting from 6 weeks post-BMT, the mice were intraperitoneally given 0.5 mg of E_2 dipropionate (Ovahormon Depot from Teikoku Hormone MFG, Tokyo, Japan) twice for 3 days. The E_2 administration was repeated every 4 weeks until 28 weeks after BMT. At 40 weeks, E_2 administration was switched so that the formerly unstimulated mice were challenged with E_2 (Group 2).

Peripheral blood counts and measurement of respiratory burst activity

A complete blood cell count (CBC) was performed using tail vein blood on a PC-608 particle counter (Erma, Tokyo, Japan) according to the manufacturer's recommendations. Blood smears were stained with Wright–Giemsa using standard methods and examined at × 500 for differential analysis.

Superoxide production by peripheral leukocytes was assayed using the NBT slide test of Buescher with slight modification.[10] Fresh whole blood from the tail vein was placed on a glass slide and incubated at 37°C in a humidified chamber until it had clotted. The clot was gently removed, and the slide was rinsed in phosphate-buffered saline (PBS) to free it of erythrocytes, then covered with NBT-saturated RPMI-1640 medium containing 100 ng/ml PMA and 5% human serum albumin. After incubation at 37°C for 20 min, the slide was rinsed in PBS, fixed in absolute methanol for 60 s, and counterstained with 1% safranine-O (Sigma) to identify nuclear morphology. Superoxide production by peripheral leukocytes was assayed using flow cytometry by loading the cells with DHR (Sigma) as described.[13,14,34] Mouse whole blood was incubated with 30 μM DHR at 37°C for 5 min and stimulated with 5 μg/ml PMA at 37°C for 30 min. After erythrocytes were lysed with Lysis buffer (150 mM NH_4Cl, 20 mM $NaHCO_3$, 1 mM EDTA), the cells were stained with a biotinylated anti-Gr1 antibody (Pharmingen) plus PE/Cy5-conjugated streptavidin (DAKO, Glostrup, Denmark) and analyzed with a FACScan. Data were statistically analyzed using the Mann–Whitney *U*-test and the paired *t*-test with StatView software (SAS Institute, Cary, NC, USA).

Acknowledgements

We thank Dr MC Dinauer for X-CGD mice, and Dr M Nakamura for 7D5 monoclonal antibody. We are also grateful to Amgen for SCF, Ajinomoto for IL-6, Chugai Pharmaceuticals for Epo and G-CSF, and Takara Bio for RetroNectin. This work was supported in part by grants from the Ministry of Education, Culture, Sports, Science and Technology of Japan, and the Ministry of Health, Labor and Welfare of Japan.

References

1 Curnutte JT, Dinauer MC. Genetic disorders of phagocyte killing. In: Stamatoyannopoulos G, Majerus PW, Perlmutter RM, Varmus H (eds). *The Molecular Basis of Blood Diseases*. W.B. Saunders: Philadelphia, 2001, pp 539–563.
2 Winkelstein JA *et al*. Chronic granulomatous disease: report on a national registry of 368 patients. *Medicine* 2000; **79**: 155–169.
3 Weening RS, Kabel P, Pijman P, Roos D. Continuous therapy with sulfamethoxazole-trimethoprim in patients with chronic granulomatous disease. *J Pediatr* 1983; **103**: 127–130.
4 The International Chronic Granulomatous Disease Cooperative Study Group. A controlled trial of interferon gamma to prevent infection in chronic granulomatous disease. *N Engl J Med* 1991; **324**: 509–516.
5 Seger RA *et al*. Treatment of chronic granulomatous disease with myeloablative conditioning and an unmodified hemopoietic allograft: a survey of the European experience, 1985–2000. *Blood* 2002; **100**: 4344–4350.
6 Horwitz ME *et al*. Treatment of chronic granulomatous disease with nonmyeloablative conditioning and a T-cell-depleted hematopoietic allograft. *N Engl J Med* 2001; **344**: 881–888.
7 Kume A, Dinauer MC. Gene therapy for chronic granulomatous disease. *J Lab Clin Med* 2000; **135**: 122–128.
8 Kamani N *et al*. Marrow transplantation in chronic granulomatous disease: an update, with 6-year follow-up. *J Pediatr* 1988; **113**: 697–700.
9 Woodman RC *et al*. A new X-linked variant of chronic granulomatous disease characterized by the existence of a normal clone of respiratory burst-competent phagocytic cells. *Blood* 1995; **85**: 231–241.
10 Buescher ES, Alling DW, Gallin JI. Use of an X-linked human neutrophil marker to estimate timing of lyonization and size of the dividing stem cell pool. *J Clin Invest* 1985; **76**: 1581–1584.
11 Pollock JD *et al*. Mouse model of X-linked chronic granulomatous disease, an inherited defect in phagocyte superoxide production. *Nat Genet* 1995; **9**: 202–209.
12 Jackson SH, Gallin JI, Holland SM. The $p47^{phox}$ mouse knock-out model of chronic granulomatous disease. *J Exp Med* 1995; **182**: 751–758.
13 Björgvinsdóttir H *et al*. Retroviral-mediated gene transfer of $gp91^{phox}$ into bone marrow cells rescues defect in host defense against *Aspergillus fumigatus* in murine X-linked chronic granulomatous disease. *Blood* 1997; **89**: 41–48.
14 Mardiney III M *et al*. Enhanced host defense after gene transfer in the murine $p47^{phox}$-deficient model of chronic granulomatous disease. *Blood* 1997; **89**: 2268–2275.
15 Malech HL *et al*. Prolonged production of NADPH oxidase-corrected granulocytes after gene therapy of chronic granulomatous disease. *Proc Natl Acad Sci USA* 1997; **94**: 12133–12138.
16 Emery DW *et al*. Hematopoietic stem cell gene therapy. *Int J Hematol* 2002; **75**: 228–236.
17 Moscow JA *et al*. Engraftment of *MDR1* and NeoR gene-transduced hematopoietic cells after breast cancer chemotherapy. *Blood* 1999; **94**: 52–61.
18 Abonour R *et al*. Efficient retrovirus-mediated transfer of the multidrug resistance 1 gene into autologous human long-term repopulating hematopoietic stem cells. *Nat Med* 2000; **6**: 652–658.
19 Neff T, Blau CA. Pharmacologically regulated cell therapy. *Blood* 2001; **97**: 2535–2540.
20 Kume A *et al*. Selective expansion of transduced cells for hematopoietic stem cell gene therapy. *Int J Hematol* 2002; **76**: 299–304.
21 Ito K *et al*. Development of a novel selective amplifier gene for controllable expansion of transduced hematopoietic cells. *Blood* 1997; **90**: 3884–3892.
22 Matsuda KM *et al*. Development of a modified selective amplifier gene for hematopoietic stem cell gene therapy. *Gene Therapy* 1999; **6**: 1038–1044.
23 Xu R *et al*. A selective amplifier gene for tamoxifen-inducible expansion of hematopoietic cells. *J Gene Med* 1999; **1**: 236–244.
24 Hanazono Y *et al*. *In vivo* selective expansion of gene-modified hematopoietic cells in a nonhuman primate model. *Gene Therapy* 2002; **9**: 1055–1064.
25 Kume A *et al*. *In vivo* expansion of transduced murine hematopoietic cells with a selective amplifier gene. *J Gene Med* 2003; **5**: 175–181.
26 Hawley RG, Lieu FHL, Fong AZC, Hawley TS. Versatile retroviral vectors for potential use in gene therapy. *Gene Therapy* 1994; **1**: 136–138.
27 Dranoff G *et al*. Vaccination with irradiated tumor cells engineered to secrete murine granulocyte-macrophage colony-stimulating factor stimulates potent, specific, and long-lasting anti-tumor immunity. *Proc Natl Acad Sci USA* 1993; **90**: 3539–3543.

28 Duke GM, Hoffman MA, Palmenberg AC. Sequence and structural elements that contribute to efficient encephalomyocarditis virus RNA translation. *J Virol* 1992; **66**: 1602–1609.
29 Pear WS, Nolan GP, Scott ML, Baltimore D. Production of high-titer helper-free retroviruses by transient transfection. *Proc Natl Acad Sci USA* 1993; **90**: 8392–8396.
30 Onodera M *et al*. A simple and reliable method for screening retroviral producer clones without selectable markers. *Hum Gene Ther* 1997; **8**: 1189–1194.
31 Zhen L *et al*. Gene targeting of X chromosome-linked chronic granulomatous disease locus in a human myeloid leukemia cell line and rescue by expression of recombinant gp91^{phox}. *Proc Natl Acad Sci USA* 1993; **90**: 9832–9836.
32 Nakamura M *et al*. Monoclonal antibody 7D5 raised to cytochrome b_{558} of human neutrophils: immunocytochemical detection of the antigen in peripheral phagocytes of normal subjects, patients with chronic granulomatous disease, and their carrier mothers. *Blood* 1987; **69**: 1404–1408.
33 Hanenberg H *et al*. Colocalization of retrovirus and target cells on specific fibronectin fragments increases genetic transduction of mammalian cells. *Nat Med* 1996; **2**: 876–882.
34 Vowells SJ *et al*. Flow cytometric analysis of the granulocyte respiratory burst: a comparison study of fluorescent probes. *J Immunol Methods* 1995; **178**: 89–97.
35 Cavazzana-Calvo M *et al*. Gene therapy of human severe combined immunodeficiency (SCID)-X1 disease. *Science* 2000; **288**: 669–672.
36 Hacein-Bey-Abina S *et al*. Sustained correction of X-linked severe combined immunodeficiency by *ex vivo* gene therapy. *N Engl J Med* 2002; **346**: 1185–1193.
37 Kume A *et al*. Selective growth advantage of wild-type lymphocytes in X-linked SCID recipients. *Bone Marrow Transplant* 2002; **30**: 113–118.
38 Hacein-Bey-Abina S *et al*. A serious adverse event after successful gene therapy for X-linked severe combined immunodeficiency. *N Engl J Med* 2003; **348**: 255–256.
39 Kohn DB, Sadelain M, Glorioso JC. Occurrence of leukaemia following gene therapy of X-linked SCID. *Nat Rev Cancer* 2003; **3**: 477–488.
40 Jin L *et al*. *In vivo* selection using a cell-growth switch. *Nat Genet* 2000; **26**: 64–66.
41 Neff T *et al*. Pharmacologically regulated *in vivo* selection in a large animal. *Blood* 2002; **100**: 2026–2031.
42 Kume A *et al*. Lymphoid reconstitution in X-linked severe combined immunodeficient mice by retrovirus-mediated gene transfer. *Proc Jpn Acad* 2002; **78**: 211–216.
43 Kume A *et al*. Long-term tracking of murine hematopoietic cells transduced with a bicistronic retrovirus containing CD24 and EGFP genes. *Gene Therapy* 2000; **7**: 1193–1199.
44 Yasueda H *et al*. High-level direct expression of semi-synthetic human interleukin-6 in *Escherichia coli* and production of N-terminus Met-free product. *Bio/Technology* 1990; **8**: 1036–1040.
45 Sekhsaria S *et al*. Peripheral blood progenitors as a target for genetic correction of p47^{phox}-deficient chronic granulomatous disease. *Proc Natl Acad Sci USA* 1993; **90**: 7446–7450.

Available online at www.sciencedirect.com
SCIENCE DIRECT®
Archives of Biochemistry and Biophysics 427 (2004) 58–67
ABB
www.elsevier.com/locate/yabbi

Biochemical and molecular biological analysis of different responses to 2,3,7,8-tetrachlorodibenzo-*p*-dioxin in chick embryo heart and liver

Nobuyuki Kanzawa,* Mariko Kondo, Tomoaki Okushima, Masatoshi Yamaguchi, Yusuke Temmei, Michiyo Honda, and Takahide Tsuchiya

Department of Chemistry, Faculty of Science and Technology, Sophia University, 7-1 Kioi, Chiyoda-ku, Tokyo 102-8554, Japan

Received 11 March 2004, and in revised form 15 April 2004

Abstract

We studied the mechanism of toxicity of 2,3,7,8-tetrachlorodibenzo-*p*-dioxin (TCDD) in the chick embryo, which is an organism highly sensitive to TCDD. TCDD was injected into egg yolks prior to embryogenesis, and eggs were incubated for 12 or 18 days. In TCDD-exposed embryos, we observed increased heart wet weight and change in the color of the liver, with abnormal fatty vesicle formation. To determine whether these effects were mediated by the aryl hydrocarbon receptor (AhR), we examined expression levels of AhR, CYP1A4, and CYP1A5. AhR was expressed continuously in the heart and liver during embryogenesis, whereas induction of CYP1A4 and CYP1A5 by TCDD was detected only in the liver. In situ hybridization study of tissue sections revealed induction of CYP1A4 in the abnormal liver tissue in which color change was not observed. To determine whether these different responses to TCDD depended on the cell type, primary cultures of chick hepatocytes and cardiac myocytes were established and 7-ethoxyresorufin-*O*-deethylase (EROD) activity was measured. Induction of EROD activity following exposure to TCDD was detected in hepatocytes but not in cardiac myocytes. Although the heart is a principal target organ for TCDD toxicity and AhR is expressed throughout embryogenesis, induction of CYP1A was not observed in the chick heart. Thus, we conclude that defects in the heart induced by exposure to TCDD occur via a different pathway than that occurring in the liver.

Keywords: AhR; Cardiac myocyte; CYP1A; Hepatocyte; TCDD

Halogenated aromatic hydrocarbons (HAHs) are ubiquitous environmental contaminants that are responsible for endocrine abnormalities in wild birds and humans. Among these chemicals, 2,3,7,8-tetrachlorodibenzo-*p*-dioxin (TCDD)[1] is the most toxic environmental contaminant. The toxic effects of TCDD can lead to wasting syndrome, carcinogenicity, teratogenicity, cardiac dysfunction, and immunodepression [1,2]. TCDD also induces abnormalities, including edema, hemorrhages, and death, in fishes [3,4], birds [5–8], and mammals [1,9]. Chicken is a highly sensitive organism and is a model to examine the effects of TCDD on developmental events [7,10,11]. Large numbers of egg-injection studies have shown that TCDD is cardiotoxic and can produce structural malformation, ventricular hypertrophy, and abnormal myocyte intracellular Ca^{2+} modulation and contractility [12–14]. Atrial natriuretic factor (ANF) is a marker for cardiac hypertrophy in adult animals [15], and increased expression of ANF has been reported in hearts of TCDD-exposed chick embryos [12]. TCDD-induced toxicities are mediated by the aryl hydrocarbon receptor (AhR) [1]. AhR is a ligand-activated transcription factor and a member of the basic helix–loop–helix/per-Arnt-Sim (bHLH/PAS) family. When a ligand such as TCDD is bound, AhR

* Corresponding author. Fax: +11-81-3-3238-3361.
E-mail address: n-kanza@sophia.ac.jp (N. Kanzawa).

[1] *Abbreviations used:* AhR, aryl hydrocarbon receptor; ANF, atrial natriuretic factor; Arnt, AhR nuclear translocator; EROD, 7-ethoxyresorufin-*O*-deethylase; GAPDH, glyceraldehyde 3-phosphate dehydrogenase; TCDD, 2,3,7,8-tetrachlorodibenzo-*p*-dioxin.

0003-9861/$ - see front matter © 2004 Elsevier Inc. All rights reserved.
doi:10.1016/j.abb.2004.04.021

translocates to the nucleus and makes a heterodimer complex with AhR nuclear translocator (Arnt). Transcriptional activation of target genes is initiated by binding of the complex to a specific region called the dioxin response element (DRE) [16,17]. The major target genes are cytochrome P450 1A1 (CYP1A1) and other CYP1A family members [18]. Two avian homologues to mammalian CYP1A1 and 1A2 that are induced by TCDD have been characterized and are designated as CYP1A4 and CYP1A5 [8,19–22]. Immunohistochemical analysis of TCDD-exposed chick embryos revealed that CYP protein was induced in various tissues, including the liver and myocardium, where AhR and Arnt co-localized [23]. Activated AhR may sequester Arnt, resulting in alteration of the Arnt-dependent pathways such as hypoxia signaling pathways and explaining the TCDD-induced abnormalities. Arnt serves as a dimer partner for a large number of transcription factors such as hypoxia-inducible factor 1a (HIF-1a) [24]. Thus, TCDD is known to mediate some teratogenic responses by binding the AhR; however, the exact induction mechanism for the cardiotoxicity is not known.

In this study, we examined the contribution of AhR expression to TCDD-induced cardiotoxicity. We found that liver was the major target of AhR-mediated TCDD toxicity in chick embryo. AhR expression was maintained at equal levels in the heart and liver during embryogenesis, but no obvious induction of CYP1A4 or CYP1A5 was detected in the heart. We conclude that TCDD affects heart and liver through different pathways during embryogenesis.

Materials and methods

Animals

White leghorn (*Gallus gallus*) fertile chicken egg (Omiya Kakin, Saitama, Japan) yolks were injected with TCDD dissolved in corn oil or with corn oil vehicle prior to incubation. Eggs were sealed with wax and incubated at 37 °C in humidified air.

TCDD exposure and morphological analysis

Eggs were injected with 1.0 pmol/g egg of TCDD (Cambridge Isotope Laboratories, Woburn, MA, USA) or vehicle (control). Control and TCDD-treated embryos were collected after appropriate incubation periods (embryonic days (E) 12 and 18). Embryos were weighed and the heart and liver were inspected. Hearts and livers then were dissected for weight and morphological analysis. Differences between treated and control embryos were analyzed by Student's t test ($P < 0.01$). For the morphological analysis, tissues were fixed overnight in 3.7% paraformaldehyde, frozen in Tissue-Tek OCT compound (Miles, Elkhart, IN, USA), and sectioned. Sections (10 μm thickness) were stained with hematoxylin and eosin and analyzed histologically.

Cell culture

Primary cultures of cardiac myocytes and hepatocytes were obtained from E12 chick embryos as described previously [13,25]. Cells were grown in Dulbecco's modified Eagle's medium (DMEM) with 10% fetal bovine serum (FBS), penicillin (100 U/ml; Sigma, St. Louis, MO, USA), and streptomycin (100 μg/ml; Meiji Seika Kaisya, Tokyo, Japan). Cells were maintained in the medium at 37 °C in a humidified atmosphere containing 5% CO_2.

EROD assay

Cells were seeded in 96-well plates at a concentration of 1×10^5 cells/well and incubated for 24 h. Thereafter, medium was removed and TCDD-containing DMEM with 5% FBS was added. Control cells were incubated in the same manner except that dimethyl sulfoxide (DMSO) instead of TCDD was added to a final concentration of 1%. After 24- or 48-h incubation, cells were washed with phosphate-buffered saline (PBS), and DMEM containing 7.4 μM ethoxyresorufin and 10 μM dicumarol with 10% FBS was added to each well. After 1 h of incubation, supernatants were transferred to new wells and the fluorescence of resorufin was measured with a Fluoroimager 595 (Amersham–Pharmacia Biotech, Little Chalfont, UK). The fluorescence intensity of each well was calculated with Kodak 1D Image Analysis Software (EDAS292, version 3.5; Eastman Kodak, Rochester, NY, USA). Intensity is given relative to control intensity with standard deviations.

Northern blot analysis

To prepare DNA probes for CYP1A4, CYP1A5, glyceraldehyde 3-phosphate dehydrogenase (GAPDH), and atrial natriuretic factor (ANF), RT-PCR was done with liver total RNA from E12 chick embryos as a template. cDNAs generated with primer pairs (summarized in Table 1) were ligated to TA-cloning vector (pGEM-T Easy, Promega, Madison, WI, USA), and the inserts were excised with *Eco*RI from isolated clones. Total RNA was isolated from heart or liver of E12 chick embryos with TriZol reagent (Gibco-BRL, Gaithersburg, MD, USA). Aliquots (20 μg) of the total RNA were electrophoresed on 1.2% formaldehyde agarose gels, and the products were transferred to nylon membranes (Hybond N^+, Amersham–Pharmacia Biotech). Samples on the membranes were hybridized according to the manufacturer's instructions (ECL Labeling and Detection System, Amersham–Pharmacia Biotech).